

République Algérienne Démocratique et Populaire Ministère de l'Enseignement Supérieur et de la Recherche Scientifique École Nationale Polytechnique



Département Métallurgie

Final Year Project Thesis for the Degree of State Engineer in Materials
Engineering

Subjects:

Study Of The Effect Of Surface Treatments On The Corrosion Resistance

Of AlMgSi Aluminum Alloys In A NaCl Environment

Presented by:

Fatima MEHAREB & Manel BADOUD

Supervisor:

Dr. M. KHALFA principal researcher CRND

Co-supervisor:

Dr. A. AMROUCHE ENP

Jury Composition:

President: Dr. K. ABADLI ENP **Examiner** Dr. C. ALOUANE ENP

Presented on 07/07/2025

ENP 2025



République Algérienne Démocratique et Populaire Ministère de l'Enseignement Supérieur et de la Recherche Scientifique École Nationale Polytechnique



Département Métallurgie

Final Year Project Thesis for the Degree of State Engineer in Materials
Engineering

Subjects:

Study Of The Effect Of Surface Treatments On The Corrosion Resistance

Of AlMgSi Aluminum Alloys In A NaCl Environment

Presented by:

Fatima MEHAREB & Manel BADOUD

Supervisor:

Dr. M. KHALFA principal researcher CRND

Co-supervisor:

Dr. A. AMROUCHE ENP

Jury Composition:

President: Dr. K. ABADLI ENP **Examiner** Dr. C. ALOUANE ENP

Presented on 07/07/2025

ENP 2025



République Algérienne Démocratique et Populaire Ministère de l'Enseignement Supérieur et de la Recherche Scientifique École Nationale Polytechnique



Département Métallurgie

Mémoire de projet de fin d'études

pour l'obtention du diplôme d'ingénieur d'état en génie des matériaux

Sujet:

Étude de l'effet des traitements de surface sur la résistance à la corrosion

des alliages d'aluminium AlMgSi en milieu NaCl.

Présenté par :

Fatima MEHAREB & Manel BADOUD

Encadrant:

Dr. M. KHALFA principal researcher CRND

Co-encadrant:

Dr. A. AMROUCHE ENP

Membres du jury: :

Président: Dr. K. ABADLI ENP **Examinatrice**: Dr. C. ALOUANE ENP

Soutenues le 07/07/2025

ENP 2025

The results of this work are a priority of the Draria Nuclear Research Center. Any partial or total publication of the results without prior authorization from COMENA will be subject to legal action."

ملخص:

في مجال تصنيع صفائح الوقود للمفاعلات البحثية، يُعدا التحكم في جودة الأسطح المعننية أمرًا بالغ الأهمية لضمان أداء عال ومتانة طويلة الأمد. يلعب التنظيف الكيميائي (التقشير) دورًا أساسيًا في إزالة الشوائب وتعديل السطح لتقليل قابلية التآكل. تهدف هذه الدراسة إلى فهم تأثير المعالجات السطحية المختلفة، سواء كانت مصحوبة أم لا بمعالجة بهيدروكسيد الألمنيوم، على السلوك الكهروكيميائي لسبائك الألمنيومAIMgSi ، وهي مادة تُستخدم بشكل شائع في تصنيع صفائح الوقود. الهدف من هذه الدراسة هو تحديد المعالجات السطحية المثلي التي تقلل من تدهور الغلاف و تحسنن مقاومته العامة للتآكل.

نتمثل المعالجة السطحية المستخدمة في هذا العمل في التخميل (passivation) عند درجات حرارة مختلفة، وتحديدًا البوهمايت عند 100 درجة مئوية والبايرايت عند 70 درجة مئوية، مع دمج تقنيات التحليل (المجهر البصري، المجهر الإلكتروني الماسح، حيود الأشعة السينية) والقياسات الكهروكيميائية. تمت دراسة تأثير المعالجات الأولية على عملية التخميل. كانت طبقة البوهمايت الناتجة عن التقشير بـ NaOHفقط أقل تغطية مقارنة بالسطح الذي خضع لعمليات التنظيف والتقشير والتعديل الكيميائي. تؤكد النتائج الكهروكيميائية أن تشكيل طبقة بوهمايت في

ظروف الأوتوكلاف المضبوطة بدقة يُحسن بشكل كبير من مقاومة التآكل لسبيكة AA6061 وقدامت طبقة البوهمايت الناتجة عن المعالجة الكاملة التي تتضمن التقشير (T3) أفضل حماية من بين جميع المعالجات المختبرة.

ا**لكلمات الرئيسية**: سبائك الألمنيوم، ظواهر التآكل، عمليات المعالجة السطحية، التقشير الكيميائي، تكوين هيدروكسيد الألمنيو_{ر.} ثلاثي هيدروكسيد الألومنيوم.

Résumé:

Dans le domaine de la fabrication des plaques combustibles pour les réacteurs de recherche, le contrôle de la qualité des surfaces métalliques est crucial pour assurer une performance élevée et une durabilité à long terme. Le décapage chimique joue un rôle essentiel dans l'élimination des impuretés et la modification de la surface pour réduire la susceptibilité à la corrosion. Cette étude vise à comprendre l'influence des différents traitements de surface combinés ou non avec un traitement par hydroxyde d'aluminium, sur le comportement électrochimique de l'alliage d'aluminium AlMgSi, un matériau couramment utilisé dans la fabrication des plaques combustibles. L'objectif de cette etude est d'identifier les traitements de surfaces optimaux qui minimisent la dégradation de la gaine et améliorent la résistance globale à la corrosion.

Le traitement de surface utilisé dans ce travail est une passivation a différente température à savoir la Boehmite et la Bayérite a 100°C et a 70°C respectivement, en combinant des méthodes de caractérisations (MO, MEB, DRX), et des mesures électrochimiques. L'influence des prétraitements sur la passivation a été étudiée. La couche de passivation de Boehmite déposée après un décapage au NaOH seul est moins couvrante que sur une surface qui a été nettoyée, décapé et neutralisé. Les résultats électrochimiques confirment que la f ormation d'une couche de boehmite dans des conditions d'autoclave soigneusement contrôlées améliore considérablement la résistance à la corrosion de l'alliage AA6061. La surface de boehmite issue du traitement complet incluant le décapage (T3) a offert la meilleure protection parmi tous les traitements testés.

Mots clés: Alliage d'aluminium, Phénomène de corrosion, Traitement de surface, Décapage, Hydroxyde d'aluminium, Trihydroxyde d'aluminium.

Abstract:

Quality control on metallic surfaces is an essential aspect of the manufacture of fuel plates for research reactors, and relates directly to optimal performance and longevity. Chemical pickling is a vital step in fuel plate production, and will remove contaminants and surface conditions which may treat corrosion inhibitors. The objective of this study is to investigate the effect of surface treatments applied either separately or together with a treatment of aluminum hydroxide, on the electrochemical behavior of AlMgSi aluminum alloy, which is the standard construction material of fuel plates. The goal of this study, based on the outcome of surface treatment protocol assessment, is to assess the optimum surface treatments for minimizing the degradation of the cladding and thereby minimizing the corrosion susceptibility.

The surface treatment used in this work is passivation at different temperatures, specifically Boehmite at 100 °C and Bayerite at 70 °C, combining characterization methods (optical microscopy, SEM, XRD) and electrochemical measurements. The influence of pretreatments on passivation was studied. The Boehmite passivation layer formed after NaOH pickling alone is less uniform than on a surface that has been cleaned, pickled, and neutralized. Electrochemical results confirm that the formation of a Boehmite layer under carefully controlled autoclave conditions significantly enhances the corrosion resistance of the AA6061 alloy. The Boehmite surface obtained from the complete treatment, including pickling (T3), offered the best protection among all the tested treatments.

Key words: Aluminum alloy, Corrosion phenomena, Surface treatment processes, Pickling, Aluminum hydroxide, Aluminum trihydroxid

DEDICATION:

Today, as I stand tall in this proud and elevated moment, I look ahead to a hopeful and successful future.

It is only right that I begin with a heartfelt word of gratitude. Above all, I thank my Lord, who was my constant companion throughout this journey granting me strength when I was weak, patience during hardships, and hope in times of despair. His presence uplifted me in silence, and his guidance carried me through out every challenge.

To my dear parents, who were my unshakable foundation, thank you for your endless support, love, and prayers. You have been the shield I stood behind when I faltered. your sacrifices will never be forgotten, and your impact on my life is eternal.

To my sisters, who embodied the roles of parents, friends, and companions words fall short of expressing how proud I am to have you in my life. Thank you for your time, patience, and unwavering encouragement, thank you Imen, Manel, Zahira, Kenza and Hadil. I can't forget my brother wahab who was a source of joy and courage.

I also extend my sincere thanks to my friends and peers, who stood by me through good times and bad ones even with a kind word or a simple smile.

Finally, A special thank for myself 'Fatima' who stumbled and rose again, who cried and laughed, who endured and overcame. Thank you for staying strong through it all, for fighting the battle of resilience.....and winning.

Fatima

To my beloved parents,

Mom and Dad, thank you for everything for your unconditional love, your strength, and all the sacrifices you've made so that I could get to where I am today. I know I can never thank you enough, but I pray that God protects you and rewards you for everything you've done for me.

To my brothers, Adem and Abd-Erraouf, my lifelong teammates thank you for always standing by me in your own quiet and solid ways.

To the one and only, my little sister Eline, the light of my life and the joy I never knew I was missing. You brought me a happiness I had waited 21 years to feel I'll carry your smile with me always.

To myself, for holding on through the challenges, for showing courage when it was hard, and for believing even when everything felt uncertain — I am proud of who I've become.

To my friends and all my family members who have supported me, encouraged me, and helped me arrive at this important chapter — thank you from the bottom of my heart.

This work is as much yours as it is mine.

Manel

ACKNOWLEDGEMENTS

We would like to sincerely thank all the professors, contributors, and individuals

who supported us throughout this work. Their guidance, remarks, and availability were of great help to us.

We express our deep gratitude to **Mr. Mohammed KHALFA** for his continuous support, valuable advice, patience, and commitment throughout the development of this thesis. His rigorous follow up and encouragement greatly contributed to the progress of our work

We would also like to thank **Mr. AHMED AMROUCHE** for his participation in the supervision of this work.

We wish to express our heartful appreciation to Dr. Kamel ABADLI, President of the jury, for

kindly agreeing to chair our defense. We are truly grateful for the attention he will give to our work. His expertise and critical insight are a real added value for us, and it is honor to benefit from his evaluation. His presence alone is a sign of trust that we deeply appreciate.

Our sincere thanks also go to **Ms. Chafia ALOUANE** for accepting to examine our thesis and to be part of the jury. We are thankful for the time and effort she will dedicate to evaluating our work.

 $m{F}_{inally, \ we \ would \ like \ to \ thank \ all \ the \ professors \ of \ the \ Department \ of \ Material}$

Engineering at the National Polytechnic School of El Harrach fir their guidance, availability, and commitment throughout our academic journey.

Thank you all, with our deepest respect and gratitude

TABLE OF CONTENTS

Table of figures	
List of tables	
Nomenclature	
General introduction	17
Chapter One : Bibliographic Study	
I-Reactors	20
I.I. What is nuclear reactor	
I.2.1 Power reactor	20
I.2.2 Research reactor	21
I.2.2.1 General design of research reactor	21
I.2.2.2.1 Type of research reactor	22
I.2.2.2.1 Heavy water reactors (HWR)	22
I.2.2.2.2 Light water reactor	22
I.3 NUR research reactor	23
I.3.1 Manufacture of fuel plate (MTR)	24
I.3.1.1 The fuel element	24
I.3.1.2 The meat of fuel element	24
I.3.1.3 The cladding	25
II. Aluminum alloys AA6061	26
II.1 Aluminum and alloys	26
II.1.1 AA60601 properties	26
II.1.2 Main characteristic of aluminum and these alloys	27
II.2 Aluminum alloy designation systems	27
II.2.1 Families of wrought alloys	28
II.2.1.1 Metallurgical state designation	29

II.3 AL alloys (6061)	30
II.4 Corrosion properties of AA6061 alloys	31
III. Corrosion	32
III.1 Definition of corrosion	
III.2 Economic aspect of corrosion	
III.3 The factors of corrosion	
III.3.3.1 Temperature	
III.3.3.2 Acidity	
III.3.3.3 Salinity regime	
III.4 Classification of corrosion	
III.4.1 Dry corrosion	
III.4.2 Wet corrosion.	34
III.5 How to avoid corrosion	34
III.5.1 Surface treatment protection	34
III.5.1.1 Surface conversion	34
III.5.1.1.1 Passivation	35
III.6 Corrosion of Al alloys	35
III.6.1 Pourbaix diagram	36
IV. AA6061 hydroxides	36
IV.1 The main hydroxide and oxides of A1	36
IV.2 Classification of AA6061 hydroxides	37
IV.2.1 Bayerite	38
IV.2.2 Boehmite	38
IV.2.3 The pseudo boehmite	38
IV.3 The multilayer structure of the hydroxide film	
V. The various forms of corrosion of Al alloys	39
V.1 Uniform corrosion	39

V.2 Localized corrosion	40
V.2.1 Galvanic corrosion	41
V.2.2 Pitting corrosion	42
Chapter Two: Experimental Part	
VI. Materials used	43
VI.1. Sample preparation	44
VI.1.1. Sample cutting	44
VI.1.2. Mechanical polishing	44
VI.1.3. Standard pickling Procedure	45
VI.1.3.1 Digressing	45
VI.1.3.2. Pickling.	45
VI.1.1.4. Autoclave	
VI.2 Characterization tools	
VI.2.1 Determination of the mass variation	
VI.2.2 Measurement of conductivity	49
VI.2.3 Measurement of the electrical contact	
VI.3 Used equipment	
VI.3.1 Ultrasonic bath	50
VI.3.2 Temperature control	
VI.3.3 Preparation of solutions	51
VI.3.3.1 Neutralization solutions	51
VI.3.3.2 Pickling solutions	51
VI.4 Characterization technique	52
VI.4 .1 Optical microscope	52
VI.4 .2 The Scanning electron microscope (SEM)	53
VI.4 .3 X-ray Diffraction (XRD)	53
VI.4 .4 Electrochemical characterization	
VI.4 .4.1 Experimental dispositive	
VI.4 .4.2 Electrochemical behavior study	
VI.4 .4.2.1 Electrochemical behavior of aluminum	55

VI.4 .4.2.2 Open circuit potential (OCP) measurement
VI.4 .4.2.3 Potentiodynamic Polarization
VI.4 .4.3 Preparation of electrolyte
VI.4.4.4 Samples preparations
Chapter Three: Experimental Results
VII.1.Observations under the optical microscope
VII.1.1 Characterization of the surface condition of the samples
VII.1.2 After pickling and oxidizing
VII.2 X-ray diffraction analysis (XRD)59
VII.3 Observation using scanning electron microscope (SEM)
VII.3.1 Boehmite layer62
VII.3.2 Beyerite layer
VII.4 Electrochemical results
VII.4.1 Open circuit potential (OCP) results
VII.4.2 Polarization curves
VII.4.2.1 Comparison of protective layer performance
VII.4.3.Observations under the optical microscope
Conclusion69
Conclusion general
References

TABLE OF FIGURES:

Figure 1: chain reaction
Figure 2: schematic of a nuclear reactor
Figure 3: top view of the hwr-hifar-reactor. Source: courtesy of ansto, australia ansto,
australia
Figure 4: osiris reactor, pool and core – credit: l. Godart, cea
Figure 5: core configuration of the nur
Figure 6: coupe longitudinal du bloc reactor nur systems
Figure 7: steps in the process of manufacturing fuel plates by "co-rolling"25
Figure 8: (a) swaged plate, (b) nozzle, (c) handling pin, (d) fuel element assembly25
figure 9: crystal structure of "face-centred cubic" aluminum
Figure 10: example of the designation of alloy 606129
Figure 11: pseudo-binary phase diagram for the 6061 system30
Figure 12: pseudo-binary diagram of the al-mg2si system31
Figure 13: representation of a local corrosion cell (local stack)
Figure 14: e-ph diagram of the al-h2o system at 25°c (m. Pourbaix)
Figure 15: phase diagram of aluminum hydroxides obtained as a result of
thermodynamic calculations and corrosion tests in demineralized water
or steam37
Figure 16: multi-layer oxide film on aluminum
Figure 17: types of corrosion (a) localized corrosion and (b) uniform corrosion40
figure 18: the different forms of localized corrosion
Figure 19: galvanic corrosion
Figure 20: evolution of the bite
Figure 21: example of used sample
Figure 22: plates before and after pickling
Figure 23: presi polisher, tech265
Figure 24: diamond paste suspension of 3 µm, then 1 µm
Figure 25: steps of mechanical polishing with four sandpapers (600, 800, 1200
and 2400)

Figure 26: the procedure and steps of pickling under a chemical fume hood
figure 27: surface state of samples after pickling
figure 28: vertical hydrothermal autoclave raectorused for surface tratemen
(beohmite >100 degrees)
figure 29: kernanalysis scale with a 200-gram range
figure 30: conductivity meter model cond 3110
figure 31: digital multimeter
figure 32:(a) ultrasonic tank, (b) acetone and ethanol for degreasing50
figure 33: magnetic heating plate
figure 34: hand-held digital thermometer
figure 35: preparation of the neutralization solution
figure 36: sigma-aldrich caustic soda crystallites
figure 37: optical microscope
figure 38: scanning electron microscope
figure 39: reflection of x-rays by a family of lattice planes spaced a distance d apart54
figure 40: showing the counter electrode, reference electrode
figure 41: photography of assembly experimental
figure 42: materials used for the preparation of $0.05 \mathrm{m}\mathrm{nacl}$ electrolyte (distilled water, chloride
sodium and a magnetic agitator)56
figure 43: kcl crystallites
figure 44: assembly preparation of samples for electrochemical tests
figure 45: optical micrographs illustrating the surface condition of the samples: (a)
mirror-polished, (b) rough state
figure 46: optical micrographs showing the surface condition of the samples (a)
polished, (b) pickled, (c) oxidized
figure 47: xrd pattern of the corrosion product obtained at 100°c for 3 days60
figure 48: xrd diagram of the corrosion product obtained at 70°c for 03 days61
figure 49: sem image and eds spectrum showing the boehmite layer formed on aa6061 after
autoclave treatment
figure 50: sem image and eds spectrum showing the bayerite layer formed on aa6061 after
autoclave treatment
Figure 51: OCP of treated samples of aluminum alloy AA6061 in a 0.05M NaCl
65
Figure 52: polarization curves of treated samples of aluminum alloy AA6061 in a 0.05M

NACL	57
Figure 53: Optical micrographs showing the surface of the samples (a) T5, (b) T3,	(c)
T46	9

LIST OF TABLE:

Table 1: the effect of alloying elements on the properties of aluminum	.27
Table 2: Designation of the main series of aluminum alloys	28
Table 3: chemical composition in mass % of the alloy's hearing elements	29
Table 4: reactions of the system aluminium in tap water.(the electrochemical reaction	in the
corrosion of aluminum)	31
Table 5: Aluminum corrosion forms due to temperature	.33
Table 6: oxide and hydroxides phases of aluminum	.38
Table 7: Chemical composition range of Alloys 6061 (ASTM B209)	43
Table 8: mass of different sample a before and after pickling	47
Table 9: mass of different sample before and after autoclave	48
Table 10: Elemental composition (%) of Boehmite	62
Table 11:Elemental composition (%) of Boehmite	64
Table 12: the results of polarization (Tafel tests) of treated samples of AA6061 alloy	67

NOMENCLATURE

• AA6061: Aluminum alloy of the Serie 6xxx

• **HWR:** Heavy water reactors

• LWR: light water reactors

• MTR: Material Testing Reactor

• CFC: face-centered cubic structure

• **ASTM**: a standard specification by the American Society for Testing and Materials

• SEM: scanning electron microscope

• XRD: X-ray diffraction

• OCP: open circuit potential

• E0: stabilization potential

• Icorr: corrosion current density

• **Rp:** polarization resistance

General Introduction

Aluminum alloys stand out from other metallic materials thanks to several advantages, such as their low cost, light weight, and adjustable mechanical strength, among others. However, corrosion remains a major issue for this material, regardless of its type. In harsh environments, a self-generated passive layer is frequently insufficient, even though it does provide some protection against atmospheric corrosion [1].

A number of strategies have been investigated to improve the corrosion resistance of aluminum alloys in these conditions, such as surface modification techniques, cold/hot working, and the creation of new alloys by incorporating rare earth elements [2].

Among these, surface modification is considered the most effective method. Anodizing, electroplating, polymer coatings, and conversion coatings have been widely studied and applied.

Recently, surface pretreatment of aluminum alloys has also been recognized as a critical step and has begun to attract considerable attention. Before the conversion treatment, aluminum alloys are typically immersed in an alkaline solution to remove oily residues and the oxide layer formed in air .followed by acid cleaning to eliminate corrosion products left behind by the alkaline degreasing process. After this pretreatment, the aluminum surface is in optimal condition to facilitate electrochemical or chemical reactions at the metal–electrolyte interface. [3-5],

Various chemical formulations have been used for alkaline degreasing, such as NaOH, Na_2CO_3 , and Na_3PO_4 . Pickling agents commonly include HNO_3 , HF, H_3PO_4 , and acetic acid. Generally, aluminum pretreatment always includes both alkaline cleaning and acid pickling steps. Some researchers have also proposed multi-step alkaline cleaning or multi-step acid pickling using mixed acid solutions as part of the pretreatment procedure. Numerous studies have focused on the effect of such pretreatments on the corrosion resistance of aluminum alloys [4].

In the research reactor, cladding has been used as vital part to protect the fissile fuel, as it forms a metallic sheath over the fuel and offers physical separation from the coolant. It also functions as a major barrier that prevents fission product leakage into the external environment. The cladding is made of AA6061 aluminum alloy to the favorable properties if offers.

Given the importance of preserving the AA6061 alloy, used as cladding in nuclear reactors, from corrosion—especially in humid environments. This work adopted surface treatments aimed at forming protective oxide layers on the alloy's surface. This was achieved through the surface treatment in an autoclave using a salt-free medium (ultrapure water) and at a pH of about 6 under controlled conditions, with the aim of forming a Boehmite layer (γ-AlOOH) at temperatures above 100 °C, or a Bayerite layer (Al (OH)3) at lower temperatures. These layers aim to provide effective corrosion protection, while maintaining a low thickness to ensure good thermal and electrical conductivity, which is necessary for the performance of the cladding inside the reactor. Efforts were also made to obtain a coherent layer, with high corrosion resistance, achieving a balance between protection and physical requirements.

The experiments were carried out studying the alloy's behavior in a medium with sodium chloride (NaCl) to test its aggression under more strenuous conditions. The effectiveness of protective layers was determined with electrochemical techniques based on voltage and current measurements.

This research was carried out as part of a project hosted at the Draria Nuclear Research Center (CRND). This thesis is organized around three chapters. Chapter 1 provides a bibliographic review of research reactors and aluminum alloys, particularly the AA6xxx series, highlighting their corrosion behavior and protection strategies. Chapter 2 describes the experimental methodology. Chapter 3 presents and discusses the results, focusing on the effectiveness of the oxide layers in corrosion prevention. The work concludes with a general summary and perspectives.

Chapter One :Bibliographic Study

CHAPTER ONE: Bibliographic study

Aluminum is widely used in reactor environments due to its low density, thermal conductivity and corrosion resistance. However, under certain conditions, especially in contact with demineralized water, Al can undergo uniform corrosion. Understanding the electrochemical behavior of Al is essential to predict and control corrosion phenomena in such system .

I. Reactors

I.1. What is a Nuclear Reactor?

Nuclear reactors are designed to initiate and sustain a controlled chain reaction (figure .1) involving the fission of fissile atoms (uranium or plutonium). Each fission event releases, on average, 2 to 3 neutrons, of which only one must induce a new fission to sustain a stable chain reaction. In addition, approximately 200 MeV of energy is released per fission event. Fission is therefore both a source of neutrons and a source of heat. The recovery of this heat is the principal objective of power reactors, where it is subsequently converted into electricity using conventional methods.

While, the utilization of the available neutrons is the main purpose of research reactors, where fuel heating is considered a constraint and, in some cases, a limiting factor in achieving high neutron fluxes [6,7].

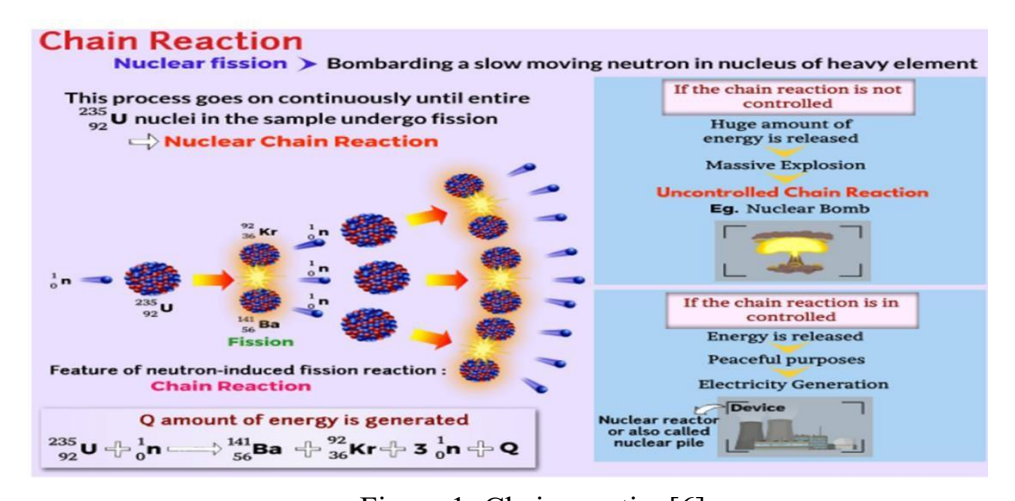


Figure 1: Chain reaction[6]

I.2. Classification of nuclear reactors

We can mention two types of this reactor which are:

I.2.1. Power reactors: providing the heat needed to turn turbines that run electric- power generators (up to 3000 MW) [8].

I.2.2. Research reactor

Research reactors are small nuclear systems mainly built to produce neutrons, not electricity like power reactors. Their design is usually simple, and they work at lower temperatures and use less fuel, which means they create less radioactive waste. These reactors are often found in research centers and universities. The output of these research reactors ranges from a few watts, such as that of a critical assembly, up to 200 MW. The neutrons they produce are useful in many areas, like production of radioisotopes for medical applications (technetium-99m, derived from molybdenum-99, is widely used for diagnosing and treating various diseases in nuclear medicine) [7], agriculture, industry, and scientific experiments. Also, because of their simple design, research reactors are very useful for training students and workers in the nuclear field, since it's easier and safer to use them for learning [9].

I.2.2.1. General Design of Research Reactors

Several key components are required for the design of a nuclear reactor:

- a fuel in which the fission reactions occur;
- a coolant, typically a liquid, that removes the heat from the reactor core;
- a moderator that slows down neutrons to enhance the probability of sustaining the chain reaction:
- a chain reaction control system, which generally includes two types:
 - control rods made of neutron-absorbing materials that can be inserted or withdrawn from the core;
 - o soluble absorbers dissolved in the coolant (such as boron in the form of boric acid) whose concentration can be adjusted over time.
- a reflector that reduces neutron leakage from the core;
- the entire assembly is surrounded by biological shielding typically made of steel and concrete designed to absorb and attenuate radiation to protect personnel and the environment outside the facility.

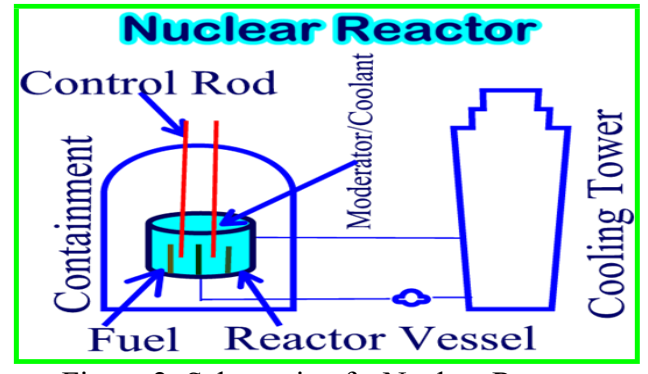


Figure 2: Schematic of a Nuclear Reactor.

I.2.2.2. Type of research reactor

There are two main types of research reactor designs, classified according to the type of coolant and neutron moderator used:

I.2.2.2.1. Heavy water reactors (HWR)

Heavy water reactors (HWR) are typically designed as "closed tank in pool" systems. They produce intense thermal neutron fluxes, extracted from the core using neutron channels, mainly for fundamental physics research.

> Heavy water possesses several remarkable properties

Due to the excellent moderating properties of heavy water, it enables the use of natural uranium, even in its oxide form, with high burn-up rates. Additionally, because its thermal properties are very similar to those of ordinary (light) water, it also serves as an effective coolant [8].



Figure 3: Top view of the HWR- HIFAR- reactor. Source: Courtesy of ANSTO, Australia ANSTO, Australia [8].

I.2.2.2.2. Light water reactors

Light water reactors are generally pool-type facilities, often with an open core. They are distinguished by their flexibility and are primarily used for the irradiation of various materials in fields, light water reactors are the most widespread, due to their simple design, moderate cost [8].



Figure 4: Osiris reactor, pool and core – credit: L. Godart, CEA[8].

I.3. NUR research reactor

The Algerian reactor NUR is an open-pool type reactor with a nominal power of 1 MW. It was commissioned in April 1989. It uses plate-type fuel elements (Materials Testing Reactor type), made of U3O8-Al enriched to 19.75%, and is cooled and moderated by light water. The reactor has vertical irradiation sites in the core and in the thermal column. It also has five horizontal irradiation channels (see figure 5) [10].

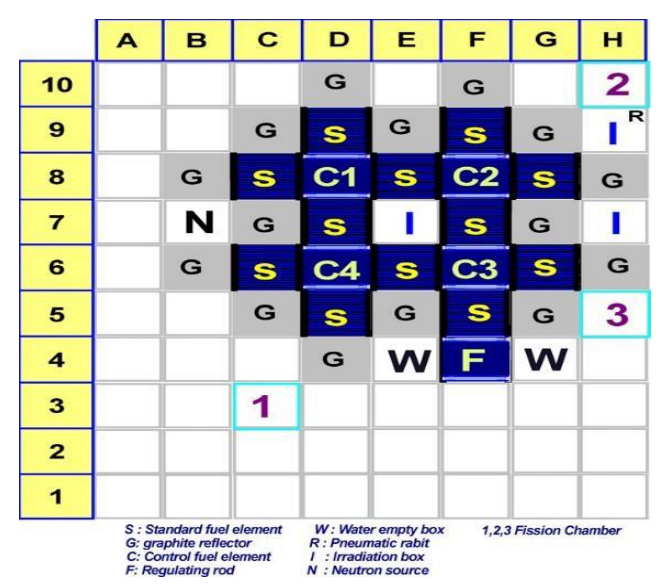


Figure 5: Core configuration of the NUR [10].

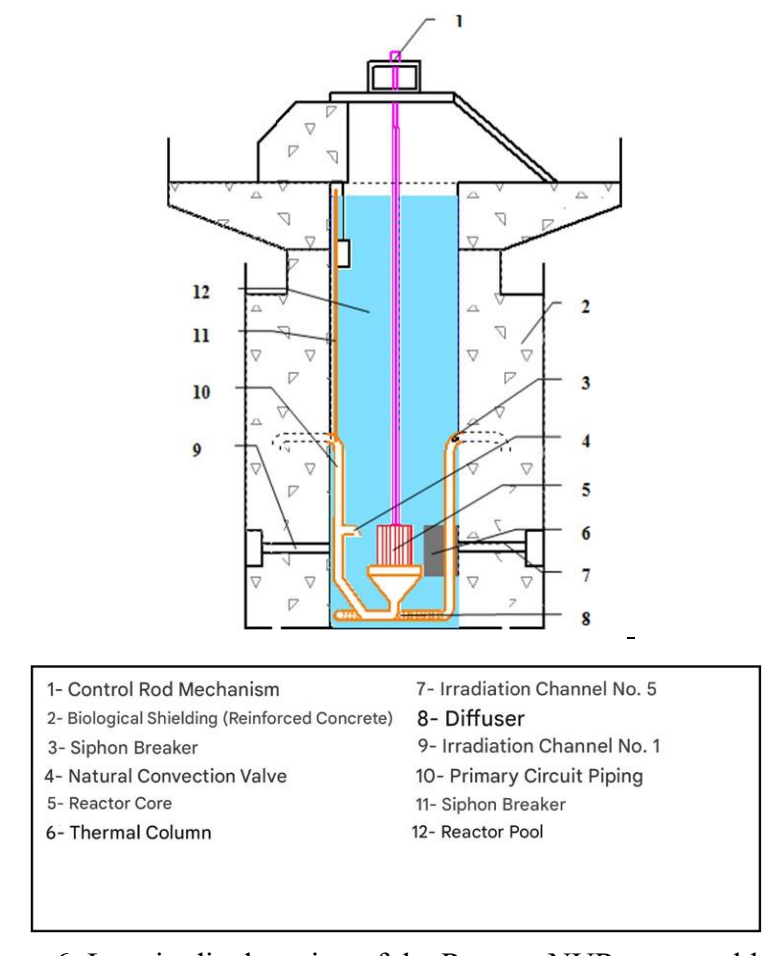


Figure 6: Longitudinal section of the Reactor NUR systems block [11].

I.3.1 Manufacture of fuel plates (MTR)

I.3.1.1. The fuel elements

Generally, the cores of pool-type research reactors can be in the form of fuel plates in the core, which is a compound based on uranium alloy (UAlx-Al, U3O8-Al, U3Si2-Al), clad in an aluminum alloy (by co-rolling) fig.7. The plates are swaged in a vertical box fig.8 that channels the cooling water, which also serves as a moderator [8].

I.3.1.2 Meat of fuel element

The fuel core is composed of a compacted powder mixture of pure Al and uranium compounds. This principle allows for the combination of properties of the two materials.

For the selected uranium compounds:

- Ability to retain fission products if the grain size is sufficient;
- Stability at temperature;
- Resistance to corrosion in water in case of sheath rupture;
- High density.

The metal matrix is chosen for its mechanical properties (the resistance of the fuel during and after manufacture), chemical properties (corrosion resistance) and thermal properties (transfer of released calories).

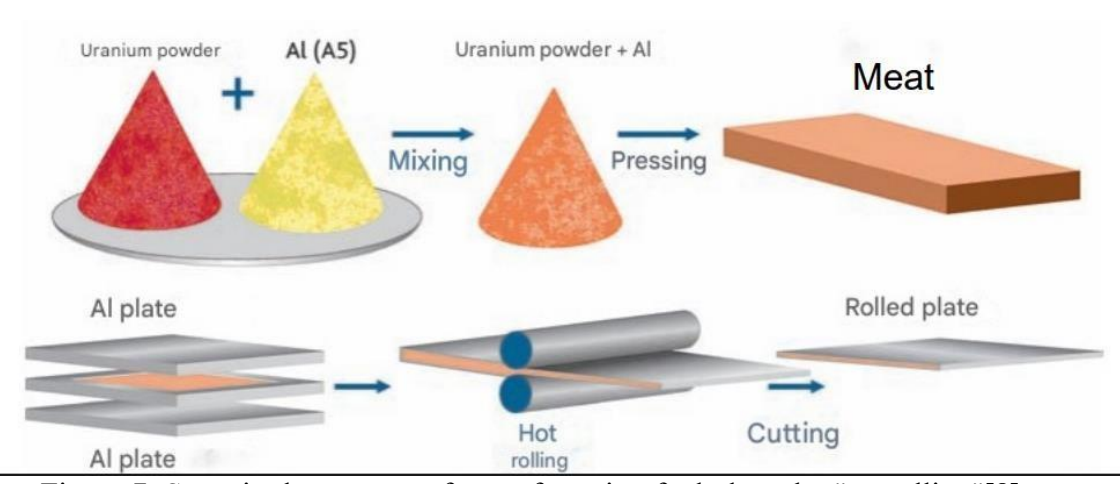


Figure 7: Steps in the process of manufacturing fuel plates by "co-rolling"[8].

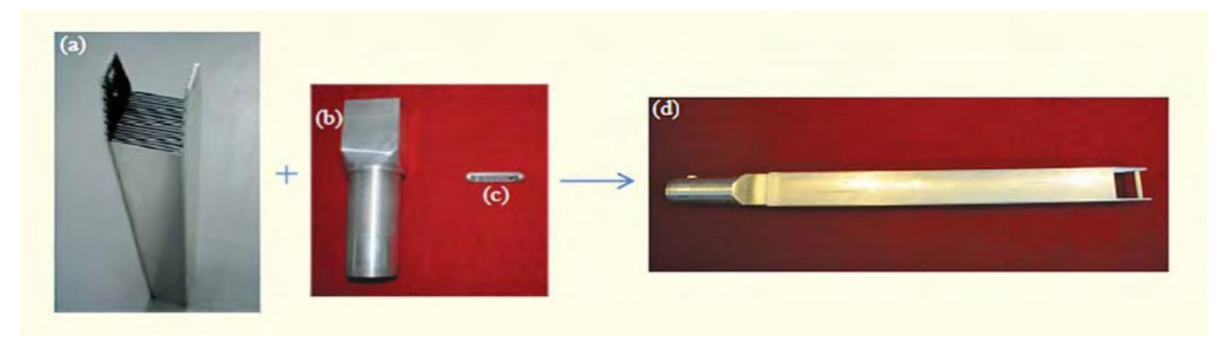


Figure 8: (a) swaged plate, (b) nozzle, (c) handling pin, (d) fuel element assembly [12].

I.3.1.3. The cladding

In a nuclear fuel, the cladding is the metallic material that envelops the fissile fuel (such as enriched uranium or its compounds). It ensures both the physical separation between the fuel and the coolant, and plays a role as a primary containment barrier against the release of fission products [13].

The clad is generally made of AA6061 aluminum alloy, due to its excellent properties:

- compatibility with the fuel;
- satisfactory thermal conductivity;
- good resistance to corrosion by the heat transfer fluid;
- a low effective cross-section so as not to diminish the core's performance;
- stable under irradiation and not to activate.

II. Aluminum alloys AA6061

II.1. Aluminum and alloys

Aluminum has an atomic symbol Al and atomic number Z=13, with face-centered cubic structure (CFC), aluminum exhibits no allotropic transformations, retaining a single solid phase and crystal structure throughout the temperature range from ambient conditions to its melting point at 660 °C) [14].

II.1.1 AA6061 Properties

Aluminum and its alloys are extensively utilized in the nuclear, aeronautical and automotive due to several specific properties [14]:

- Lightness: the density of aluminum is 2.7 g/cm ³ compared to 7.86 g/cm ³ for iron;
- Good thermal conductivity: it is 237 W/m/K for 99% pure aluminum compared to 26 W/m/K for stainless steel at 20°C;
- Good electrical conductivity: it is 3.77*10⁷ S/m for 99% pure aluminum compared to 10⁷ S/m for iron at 20°C;
- In the nuclear field, aluminum alloys are also used for their low activation under neutron irradiation and their transparency to neutrons. Indeed, the absorption cross section for thermal neutrons (E = 0.025 eV) is 0.23 barn for aluminum compared to 2 barns for iron [15];
- Good resistance to atmospheric corrosion;
- Low electrical resistivity: $0.0265 \mu\Omega$.ma 20° C;
- To improve the mechanical properties of aluminum, alloying elements are added. For example, the mechanical strength Rm of 99% pure aluminum is 120 MPa (alloy 1050), while for 6061-T6, whose main alloying elements are magnesium and silicon, it is 310 MPa [16].

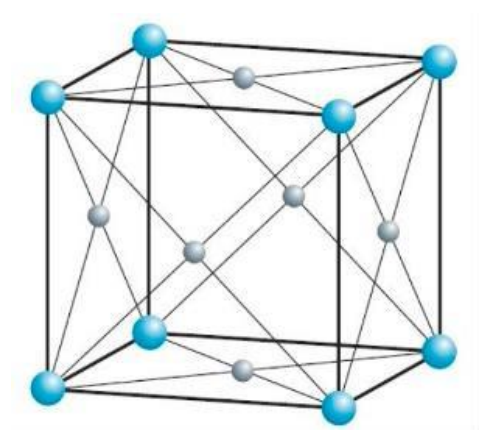


Figure 9: Crystal structure of "face-centered cubic" aluminum.

II.1.2. Main characteristics of aluminum and these alloys

The mechanical, physical and chemical properties of aluminum alloys depend on the composition and microstructure. The addition of selected elements to pure aluminum greatly improves its properties and utility (see table 1). For this reason, most applications for aluminum use alloys with one or more elemental additions.

The main alloy additions used with aluminum are magnesium, silicon, copper, manganese and zinc; other elements are also added in smaller quantities for the refinement of the grain and to develop special properties. The total quantity of these elements can make up to 10% of the alloy's composition.

Elements of impurity are also present, but their total percentage is usually less than 0.15% in the aluminum alloys [14].

Table 1: the effect of alloying elements on the properties of aluminum[17].

Elements	Effects
Magnesium	 ✓ Improves the mechanical strength of alloys. ✓ Improves corrosion resistance. ✓ Increases hardness during heat treatments. ✓ Harmful to anodizing
Silicon	 ✓ Improves forming (casting) characteristics. ✓ Greatly increases fluidity, ✓ Increases resistance to hot cracking ✓ Increases the flow characteristics of the liquid metal.
Copper	 ✓ Improves friction and mechanical characteristics. ✓ Increases mechanical strength. ✓ Improves machinability. ✓ Reduces corrosion resistance. ✓ Reduces deformation ability.
Iron	 ✓ Increases resistance to hot cracking. ✓ Reduces the tendency of the alloy to stick or weld to the mold walls. ✓ Reduces ductility

II.2. Aluminum alloy designation systems

Aluminum alloys are classified according to their manufacturing process and alloying elements. They are divided into two main categories:

- cast alloys (formed by casting);
- wrought alloys (formed by forging techniques such as rolling, extrusion, etc.).

we focus only on wrought aluminum alloys, only their designation is detailed below. The

designation of wrought alloys is governed by the ASTM B209-B209M standard [18]. This standard identifies the different alloys using a four-digit numerical designation based on their chemical composition. The first of the four digits is used to classify the alloys into eight series based on the main alloying elements. These series are detailed in Table 3. The other three digits are used to identify the alloy. The letter and number following these four digits symbolize the metallurgical treatment undergone by the alloy.

For example, 6061-T6 is a 6xxx series alloy whose main alloying elements are magnesium and silicon. T6 signifies hardened by heat treatment: solution treatment, quenching, then tempering [14].

Series Designation		Main alloying element	Main phases present in the alloy
1000	1XXX	99% Aluminum.	-
2000	2XXX	Copper (Cu).	Al ₂ Cu, Al ₂ Cu/Mg
3000	3XXX	Manganese (Mn).	Al ₂ Mn
4000	4XXX	Silicon (Si).	
5000	5XXX	Magnesium (Mg)	Al₂Mg2
6000	6XXX	Magnesium (Mg) and Silicon (Si).	Mg ₂ Si
7000	7XXX	Zinc (Zn).	$MgZn_2$
8000	8XXX	Other element.	-
9000	-	Not used	-

Table 2: Designation of the main series of aluminum alloys [14].

II.2.1. Families of wrought alloys

A four-digit numerical designation system is used to identify aluminum wrought and aluminum alloys, The first digit of the four-digit designation indicates the group [14]:

- for series 2xxx to 8xxx (see figure 10), the alloy group is determined by the alloying element present in the highest average percentage;
- the 6xxx series alloys are an exception to the rule in which the proportions of magnesium and silicon available to form silicide of magnesium (Mg_2Si) are predominant.

In alloy groups 2xxx to 8xxx, the second digit of the designation indicates the modification of the alloy. If the second digit is zero, it indicates the original alloy; Integers 1 to 9, assigned consecutively, indicate changes in the original alloy. Explicit rules have been established to determine whether a composition is simply a modification of a previously registered alloy or if it is of an entirely new alloy. The last two of the four digits of groups 2xxx to 8xxx have no particular meaning, but only serve to identify the different aluminum alloys of the group [19].

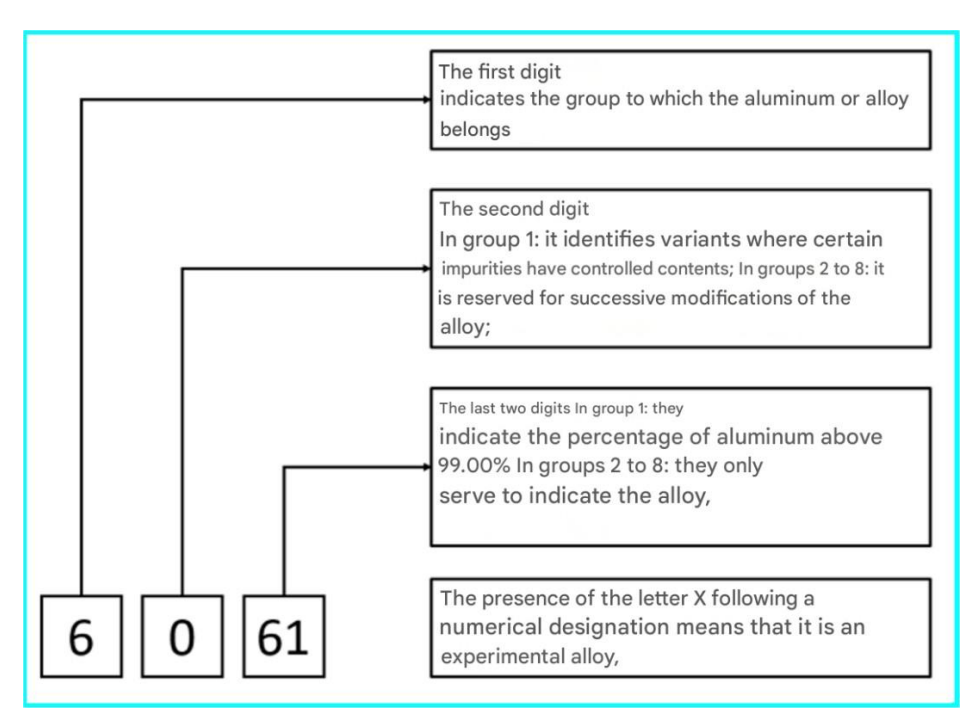


Figure 10: Example of the designation of Alloy 6061[19].

II.2.1.1. Metallurgical state designations

Common metallurgical state designations and sequence descriptions operations used to produce them are [20]:

F represents as manufactured;

O stands for annealed. Applies to wrought products; H stands for stress hardened (wrought products only); W stands for heat-treated solution;

T stands for heat-treated solution This applies to alloys with a strength of stable within a few weeks of the solution heat treatment. The T is always followed by one or more digits.

II.2.1.2. Designation table

Chemical composition specific to aluminum alloy 6061 is given Ref as a percentage by weight in table 3:

Table 3: chemical composition in mass % of the alloy's hearing elements[18].

Wt (%)	Si	Mg	Cu	Fe	Cr	Mn	Zn	Ti	Autres	Al
Min	0.4	0.8	0.15	-	0.04	-	-	-	-	98.61
Max	0.8	1.2	0.4	0.7	0.35	0.15	0.25	0.15	0.20	95.8

The first digit of the aluminum alloy designation, "6," means that the alloy of Al Contains magnesium and silicon. The relative weight percentages (weight percentages) are given by the third and fourth digits, where "6" means that there is 0.6% by weight of Si and "1" means that there is 1.0 by weight. % Mg, respectively. The second digit "0" means no other alloying elements were used. The three elements Al, Mg, and Si together form a two-phase Al alloy since Mg and Si form the single phase or compound Mg_2Si [21].

The first digit of the aluminum alloy designation, "6," means that the alloy of Al contains magnesium and silicon. The relative weight percentages (weight percentages) are given by the third and fourth digits, where "6" means that there is 0.6% by weight of Si and "1" means that there is 1.0 by weight. % Mg, respectively. The second digit "0" means no other alloying elements were used. The three elements Al, Mg, and Si together form a two-phase Al alloy since Mg and Si form the single phase or compound Mg_2Si [21].

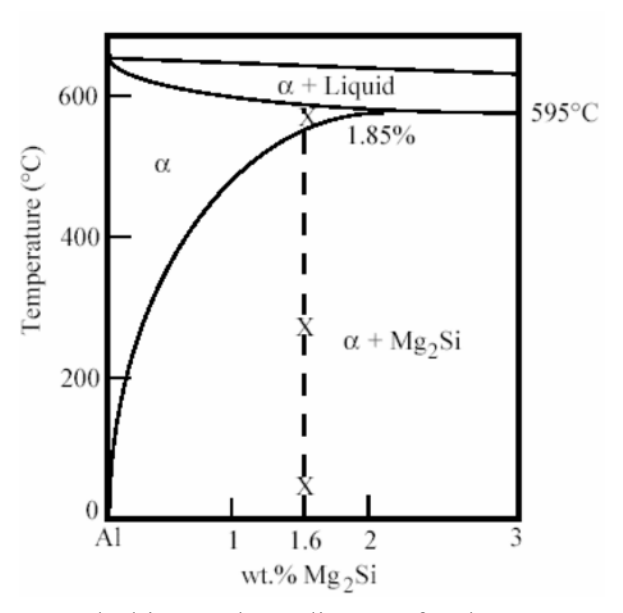


Figure 11: Pseudo-binary phase diagram for the 6061 system[22].

II.3. Al alloy (6061)

The alloys of the 6xxx series contain silicon and magnesium in approximately proportional proportions required for the formation of magnesium silicide (Mg_2Si) (see figure 11), making them treatable thermally. Magnesium and silicon are added either in equilibrium is equivalent to forming Al-Mg quasi-binary Si alloys (Mg: Si 1.73:1), or with excess silicon greater than that necessary to form (Mg_2Si) . While they are not as strong as most 2xxx and 7xxx alloys, 6xxx series alloys have good formability, weldability, Machinability and corrosion resistance with medium strength.

The alloys in this heat-treated units can be formed in the T4 state (treated solution thermally treated but not heat-treated by precipitation) and reinforced after formation at full T6 (heat-treated solution plus precipitation heat treatment) [23].

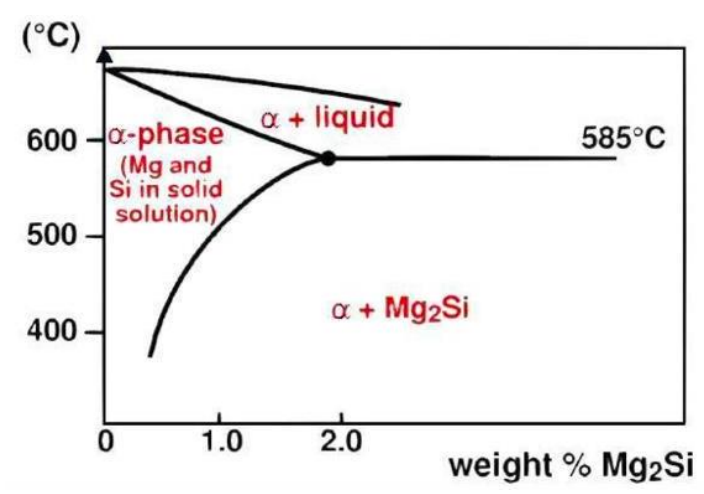


Figure 12: Pseudo-binary diagram of the Al- Mg_2Si system[23]

-

II.4. Corrosion properties of AA6061 alloys

Corrosion of metals is an electrochemical reaction which involves oxidation of the anode into a positive ion, which is released from the solid metal (R1) (Table 4). The oxidation is coupled with a reduction reaction. In the system aluminum and water, the metal is the anode and the water is the electrolyte. Cathodic reactions common in the system are reduction of hydrogen ions to hydrogen (R2) and reduction of oxygen to either hydroxide (R3) (in alkaline or neutral media) or water (R4) (in acidic media). Copper ions from the water can also be reduced (R5). The oxidized aluminum results in $Al\ (OH)_3$ (R6), which is insoluble in water and precipitates as a white gel [24].

Table 4: reactions of the system aluminum in tap water. (The electrochemical reaction in the corrosion of aluminum)[25]:

Oxidation:	$Al \to Al^{3+} + 3e^{-}$	[1]
	$2H^+ + 2e^- \rightarrow H_2$	[2]
Reduction:	$O_2 + 2H_2O + 4e^- \rightarrow 4OH^-$	[3]
	$O_2 + 4H^+ + 4e^- \rightarrow 2H_2O$	[4]
	$Cu^{2+} + 2e^- \to Cu$	[5]
Forming of corrosion product:	$Al^{3+} + 3OH^{-} \rightarrow Al(OH)_{3}$	[6]

III. Corrosion

III. 1. Definition of corrosion

Corrosion is generally defined as the deterioration or degradation of the properties of a metal or alloy due to chemical, electrochemical, or biological reactions [26,27]. It can occur in various types: Chemical corrosion results from a heterogeneous reaction between the metal and a dry gas or non-conductive liquid without electric current.

Biocorrosion corresponds to the set of modifications of the physicochemical and mechanical properties of a material under the action of microorganisms (bacteria, fungi, algae) [28,29]. The most common type is electrochemical corrosion, which takes place in aqueous environments and involves an electrochemical reaction between the surface of a material and an electrolyte. This type of corrosion is characterized by the formation of cells through which electric current flows, and it involves both a chemical reaction and the transfer of electric charges (the flow of a current). This corrosion requires the presence of a reducing agent (H_2O , O_2 , H_2 , etc.), without which the corrosion process cannot proceed [28]. This phenomenon corresponds to a redox reaction, consisting of [30]:

• The oxidation reaction of a metal known as the "anodic":

$$Mn \rightarrow Mn^{x^+} + xe^{-1}$$
 (I.1)

• The reduction reaction of an oxidizing agent is called a "cathodic":

This reaction (I.1) is necessarily coupled with a cathodic reaction (of reduction).

- In an acidic medium: $3H^+ + 3e^- \xrightarrow{3} _{2}H_2$
- In a basic or neutral medium: $O_2 + 2H_2O + 4e^- \rightarrow 4OH^-$

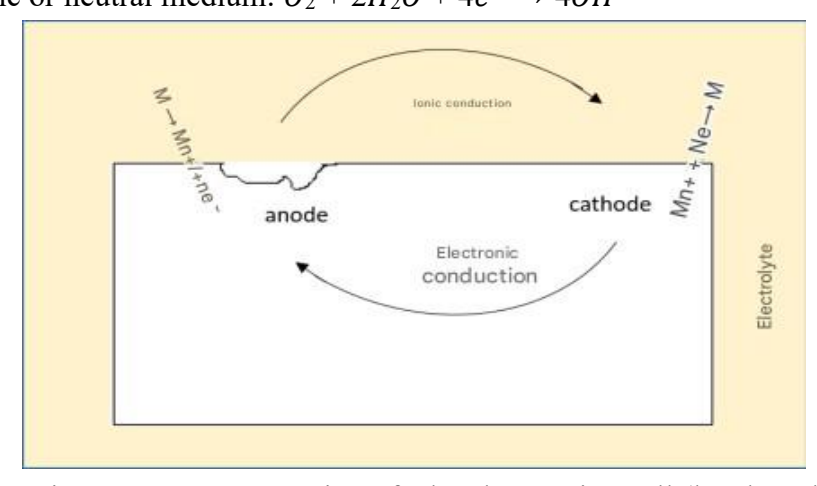


Figure 13: Representation of a local corrosion cell (local stack)[30].

III. 2. Economic aspect of corrosion

Corrosion affects a wide range of critical sectors such as aerospace, automotive, marine and nuclear industries where it poses serious threats to the safety, durability, and performance of metallic systems. Therefore, the main objective of studying corrosion is primarily economic. It's true that there are almost no cases where control of corrosion can be talked about, because level zero, or no corrosion(...)), is an unreachable goal. Some of the measures that help in controlling corrosion are too costly compared to the equipment being guarded. the direct or indirect effects of corrosion can be summarized as follows [31,32]:

- 1. Reduction or halt in production;
- 2. cost of maintenance and inspection;
- 3. cost due to the use of more noble materials;
- 4. contamination of the product by soluble corrosion products;
- 5. Reduction in system efficiency.

III.3. The factors of corrosion

Most pure metals are not thermodynamically stable. When exposed to the atmosphere, they form a superficial oxide layer that may be more or less protective. If this surface layer becomes weakened or damaged, the metal may undergo uncontrolled corrosion, depending on several factors [33]. These factors are summarized in:

III.3.1. Temperature

Generally, an increase in temperature accelerates corrosion phenomena by decreasing the stability domains of metals and speeding up the kinetics of reactions and mass transport(see table 5). However, the significance of this influence varies depending on the corrosive environment in which the material is found [28,34].

Table 5: Aluminum corrosion forms due to temperature [33].

Temperature domain	Corrosion form	
≤ 100°C	Pitting corrosion	
100-150°C	Uniform corrosion	
150-250°C	Uniform corrosion and Intergranular corrosion	
≥250°C	Intergranular corrosion and metal destruction	

Chapter One: Bibliographic Study

III.3.2. Acidity

The susceptibility of the material to corrosion depends on the pH of the electrolyte. A high concentration of protons in the solution increases the aggressiveness of the environment, which alters the balances of chemical and electrochemical reactions. Corrosion increases with the decrease in the pH of the environment [28,35].

III.3.3. Salinity regime

Chlorides are aggressive ions, often responsible for localized corrosion; their presence in solutions is accompanied by complementary effects. On one hand, their local concentrations induce acidification of the environment, and on the other hand, salinity influences the conductivity of the aqueous medium [28,36].

III. 4. Classification of corrosion

Corrosion develops according to two processes:

III.1.1. Dry corrosion

Dry corrosion refers to the degradation of materials in the absence of moisture. it usually takes place when a metal comes into contact with gaseous environment at high temperatures (sup of 200c°). It plays a very important role in devices that works in hot environments like engines or turbines [27].

III.1.2. Wet corrosion

it can appear in systems involving a metal and another material, the medium consists of a liquid or humid vapor (electrolytic) at moderate temperature, leading for example to the breakdown of organic materials or even concrete[27].

III. 5. How to avoid combat corrosion:

The methods of protection and prevention against corrosion are as follows [31]:

- prevention through a judicious choice of materials;
- protection by corrosion inhibitors;
- electrochemical protection;
- surface treatment protection.

III.5.1. Surface treatment protection

It is carried out either by surface conversion or by applying an exterior coating.

III.5.1.1. Surface Conversion

The different conversion layers depend on the manufacturing process, passivation, anodization, phosphating, and chromating.

III.5.1.1.1. Passivation

When aluminum is treated with concentrated nitric acid, its surface undergoes changes that make it non-reactive to less concentrated solution. This phenomenon is known as passivation. In simple terms, passivation refers to the formation of a thin metal oxide layer on the surface of the metal, which acts as a protective barrier, preventing direct contact between the metal and its surrounding environment [37].

III.6. Corrosion of Al alloys

Aluminum exposed to air immediately forms a transparent layer of alumina (Al₂O₃) with 5 to 10 nanometer depth to protect the metal from oxidation (equation 1). The oxide film is relatively stable in aqueous solution. The film does not have the same resistance in alkaline and acidic solutions. Generally, the corrosion of aluminum is based on the following electrochemical oxidation and reduction half-reactions [38].

$$4Al + 3O_2 \rightleftharpoons 2Al_2O_3 \dots 1$$

 $2HO_2+O_2 + 4e^- \rightarrow 4OH^-+O_2$
 $Al \rightarrow Al^{3+} + 3e^{-1}$
 $Al + 3H_2O \rightleftharpoons Al(OH)_3$

III.6.1. Pourbaix diagram:

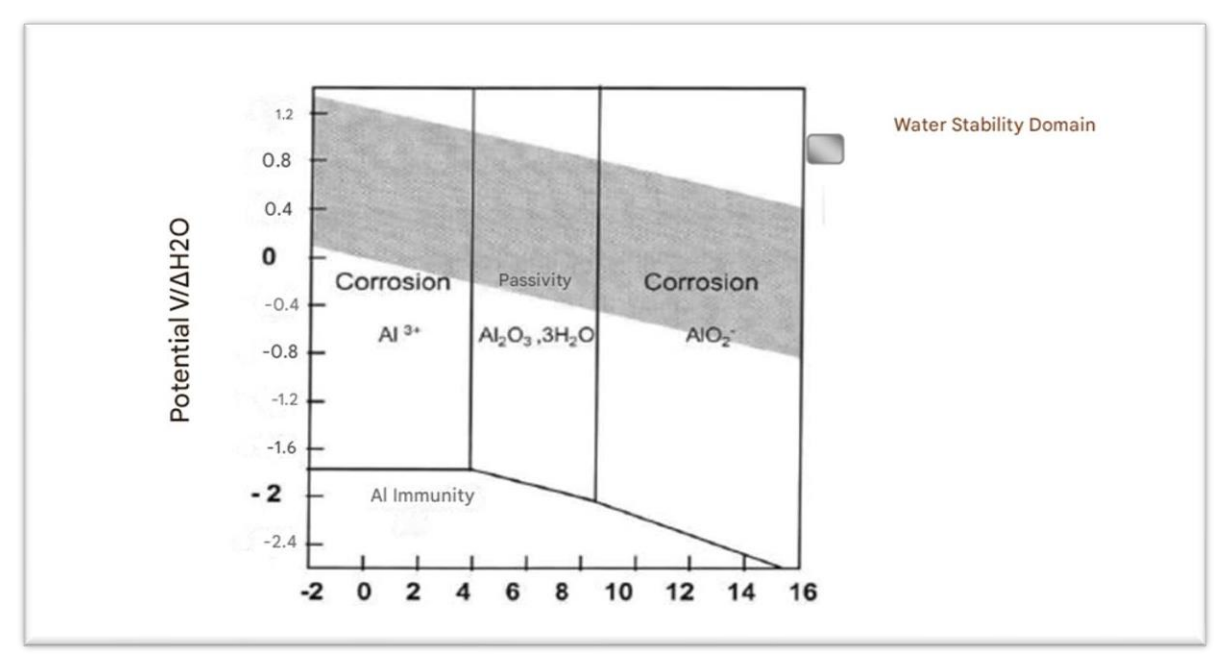


Figure 14 : E-pH diagram of the Al-H₂O system at 25°C (M. POURBAIX)[40].

From the Pourbaix diagram (figure 14), we can study the stability of the aluminum surface as a function of pH. The Pourbaix diagram of aluminum consists of 4 domains corresponding to three distinct states:

- passivation, if the metal can be covered by an insoluble oxide or hydroxide.
- a corrosion, if there is a soluble corrosion product.
- immunity, if it is in conditions where it cannot be corroded (the ion concentration is $< 10^{-6}$ M).

In solutions (4 < pH < 9), an oxide film protects the metal (passivation). Aluminum is only corroded homogeneously in a very acidic solution, with the formation of Al^{+3} , or in an alkaline solution, with the formation of aluminates (AlO^{-2}).

The resistance and stability of the oxide layer depend on the ambient environment, the composition of the alloy, and the microscopic structure of the metal (depending on the thermal treatments applied). The electrochemical behavior of aluminum is influenced by the natural oxide film that governs the corrosion resistance of aluminum [39,40].

IV.AA6061 hydroxides

IV.1. The main hydroxides and oxides of aluminum

The crystalline phase of aluminum hydroxide depends on the pressure and temperature of the aqueous medium.

Under the conditions of interest for this study, the maximum temperature is between 70 and superior to 100°C. Under these conditions, according to the aluminum hydroxide phase diagram (Figure 15) [41], bayerite and boehmite are likely to form.

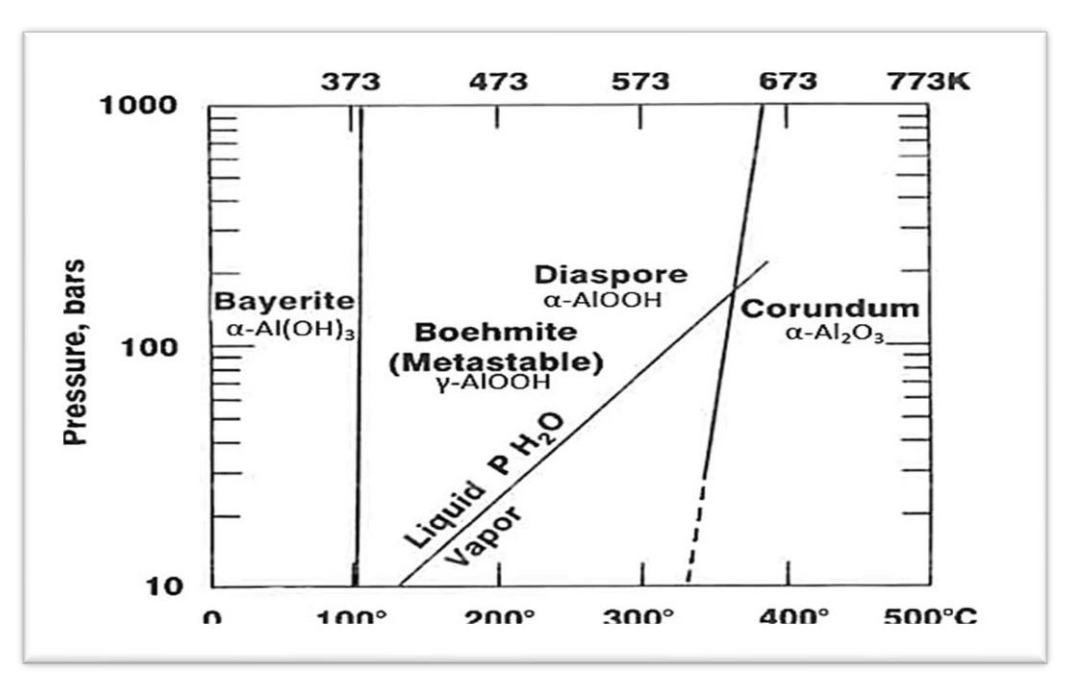


Figure 15: Phase diagram of aluminum hydroxides obtained as a result of thermodynamic calculations and corrosion tests in demineralized water or steam [41].

IV.2. Classification of AA6061 hydroxides

Depending on the physicochemical conditions, several products resulting from the interaction between Aluminum and water have been listed:

- alumina trihydrate, Al $(OH)_3$ (aluminum trihydroxide) in several solid phases: bayerite, gibbsite et nordstrandite;
- alumina monohydrate, AlOOH (aluminum oxyhydroxide): boehmite and diaspore;
- anhydrous alumina, Al_2O_3 (aluminum oxide): corundum.

All of these products are crystalline solids. A poorly crystallized structure of oxyhydroxide, named pseudo-boehmite or gelatinous boehmite, seems to be the compound formed initially over a wide range of temperatures and pressures, of these different solids. The transformations between these different oxide phases result from recrystallization processes and dehydration depending on the temperature and pressure conditions [42] (see table 6).

Variété	Réseau cristallin	Désignation chimique	Formule chimique	Température de formation	Densité
Alumine amorphe		oxyde d'aluminium	Al ₂ O ₃	< 50-60°C	3,40
Bayérite	monoclinique	trihydroxyde d'alumine	α -Al(OH) ₃	60-90°C	2,53
Boehmite	orthorhombique	hydroxyde d'aluminium	у-АІООН	> 90°C	3,01
Corindon	hexagonal	oxyde d'aluminium	α-Al ₂ O ₃	> 350°C	3,98

Table 6: oxide and hydroxides phases of aluminum [43].

IV21. Bayerite

It is a rare, naturally occurring mineral form of aluminum trihydroxide (Al (OH)₃), typically synthesized in the laboratory. It can be prepared through several methods, including the treatment of aluminum chloride with cold ammonium hydroxide, neutralization of sodium aluminate with CO₂ at low temperatures, or hydrolysis of aluminum alcoholates below 40°C. Its crystal structure is composed of Al-OH octahedral layers arranged in an AB-AB sequence, similar to gibbsite but with distinct stacking and symmetry—likely orthorhombic.

Bayerite usually forms somatoid particles (uniform shapes without crystal faces) and is commercially produced for high-purity applications such as catalyst manufacturing [44].

IV22. Boehmite

One way to improve the corrosion resistance of aluminum is to modify the natural oxide (Al_2O_3) . The oxide film gives aluminum a good corrosion resistance compared with the expectations from the sequence of electrochemical potentials. The surface properties depend on the composition and structure of the oxide layer. Boehmite (AlOOH) is formed in water environment at a temperature superior to 100° C [45-47].

Boehmite can be synthesized by neutralizing aluminum salts or aluminates at or above boiling temperature, or by treating activated aluminum with hot water. It also forms via solid-state transformation of gibbsite when heated between ~380–575 K. Structurally, boehmite has an orthorhombic lattice, with hydrogen atoms asymmetrically located between oxygen layers. It is commercially important as a precursor to activated alumina used in catalysts and adsorbents [44].

IV23. The pseudo-boehmite

In the literature, pseudo-boehmite is described as a gel of inhomogeneous structure and composition. This hydroxide is a nanocrystalline phase.

The crystalline lattice of boehmite is composed of two atomic planes of AlOOH. The two planes are linked by hydrogen bonds [41]. In pseudo-boehmite, the boehmite lattice is deformed: water molecules are intercalated between the two atomic planes of AlOOH [48]. As a result, the boehmite is hydrated, up to 30% by mass of the hydroxide is water. The level

of hydration depends on the history of the sample [41]. During an X-ray diffraction analysis, the lines of this gel are close to those of boehmite [49].

IV.3. The Multilayer structure of the hydroxide film

In aqueous corrosion tests at a temperature between 50 and 250°C, the formation of an aluminum hydroxide film is observed on the surface of the samples. This film is made up of three distinct layers. The three layers of the film are [41] (see figure 16):

- a compact inner layer of pseudo-boehmite in contact with metal.
- a crystalline outer layer (boehmite or bayerite depending on the temperature of the test), in contact with the solution.
- a thin intermediate layer of boehmite nano crystallites, sandwiched between the two previous layers.

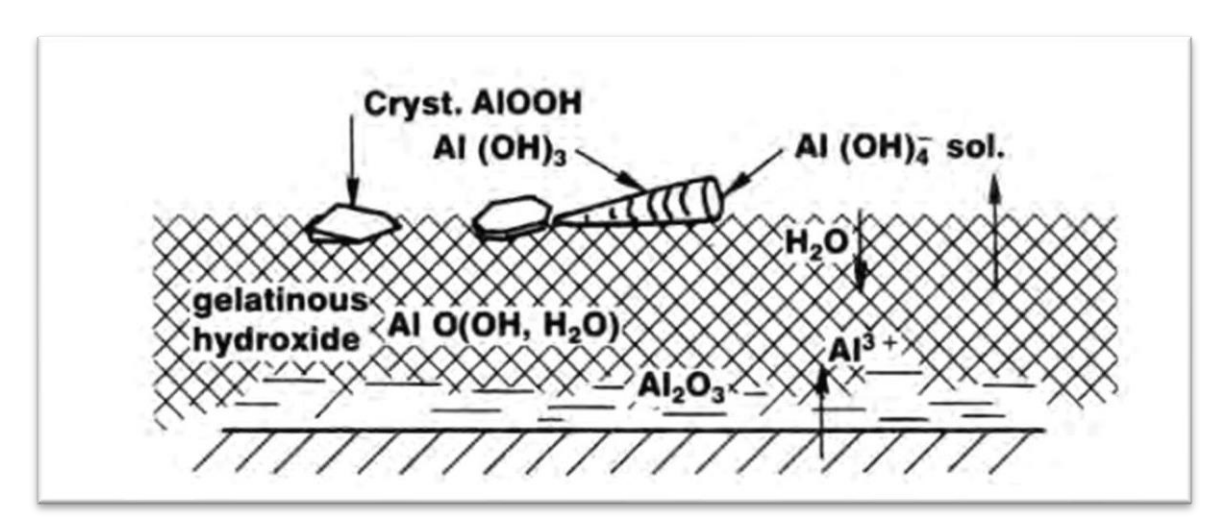


Figure 16: multi-layer oxide film on aluminum [43].

V. The various forms of corrosion of aluminum alloys

Two broad categories of corrosion are recognized:

- general (uniform) corrosion: a consistent and widespread thinning of the material surface.
- localized corrosion: occurs in small, specific areas of the metal. The following section outlines the main forms of both uniform and localized corrosion found in aluminum alloys, along with their defining characteristics.

V.1 Uniform corrosion

Typically begins as small pits, with a diameter of the order of micrometers, and is characterized by a uniform reduction in thickness across the entire surface of the metal: the oxide layer being dissolved in a regular manner by the corrosive agent in a natural, rural, or marine atmosphere. The corrosion rate of aluminum is extremely low, even

negligible. It does not exceed 5 μ m/year. This type of corrosion is observed in acidic or alkaline environments. In these environments, the dissolution of the natural oxide layer is quite high compared to the formation of the aluminum oxide or hydroxide layer for a given pH [37-40].

V2. Localized corrosion

often arises as a progression from uniform corrosion, typically through galvanic coupling between heterogeneous zones. It only takes a small anodic area and a large cathodic area to produce very high local penetration rates. These local heterogeneities may originate from inherent features in the metal or from variations in the corrosive environment. Unlike uniform corrosion, anodic and cathodic areas are clearly separated in localized corrosion. This type of corrosion cannot be evaluated by weight loss or overall thickness reduction. Instead, metallographic analysis and electrochemical measurements must be carried out (figure 17 and 18)

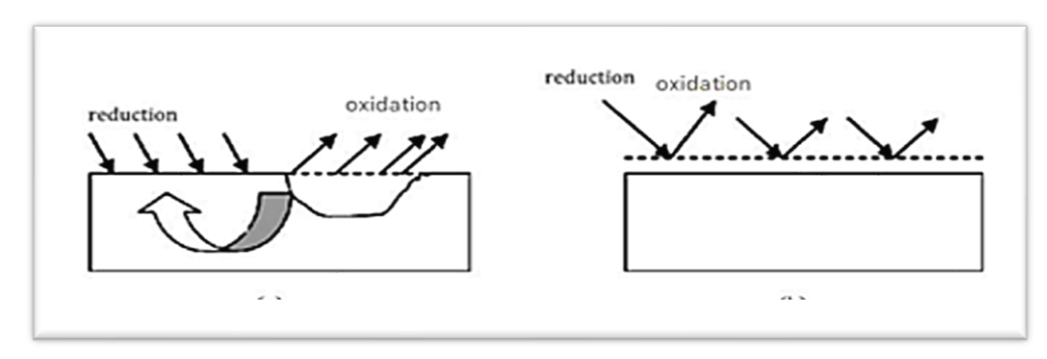


Figure 17: Types of corrosion (a) localized corrosion and (b) uniform corrosion) [33].

For localized corrosion, we distinguish several types that we can schematize as follows:

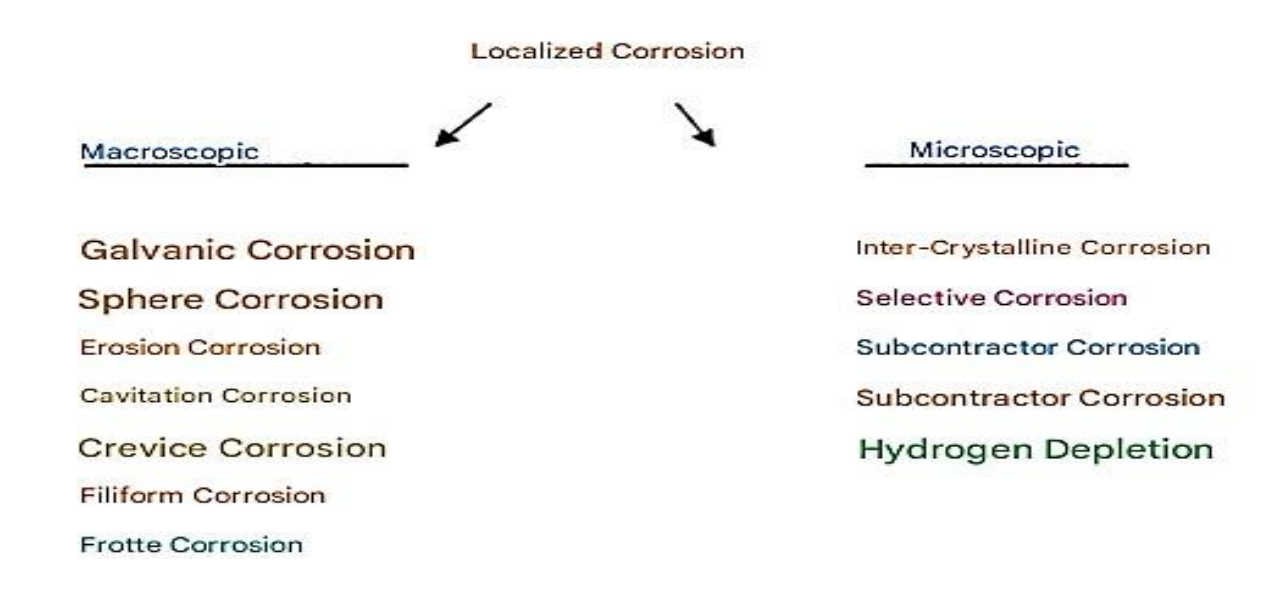


Figure 18: The different forms of localized corrosion) [33].

V21 Galvanic corrosion

This phenomenon, also known as bimetallic corrosion, occurs due to the formation of an electrochemical cell between two different metals through either electrical or electrolytic contact (see figure 19) The less noble metal acts as the anode and undergoes accelerated degradation, while the more noble metal remains protected as the cathode [38].

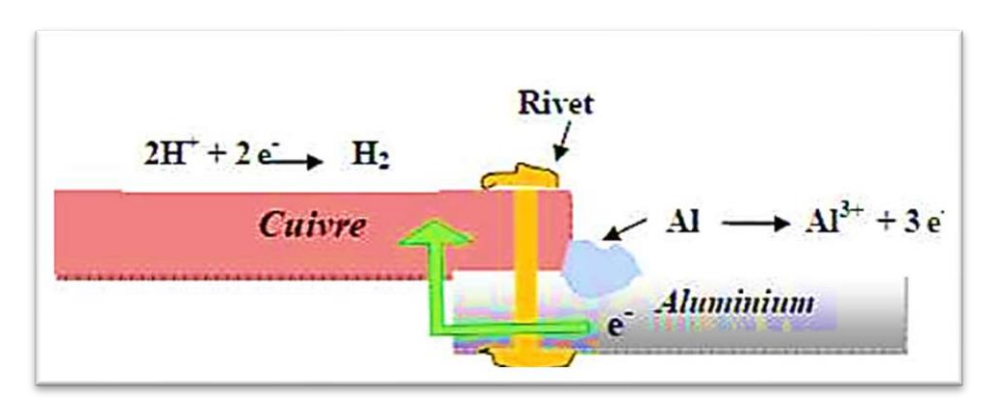


Figure 19: Galvanic corrosion [23].

V2.2. Pitting corrosion

Pitting corrosion refers to a localized attack on a passive surface; it requires the presence of aggressive anions such as Cl⁻, Br⁻, and I⁻, and an oxidant. It manifests through the

formation of small cavities (pits)(figure 20), while the passive surface remains intact. The number and shape of corrosion pits vary according to the experimental conditions[33].

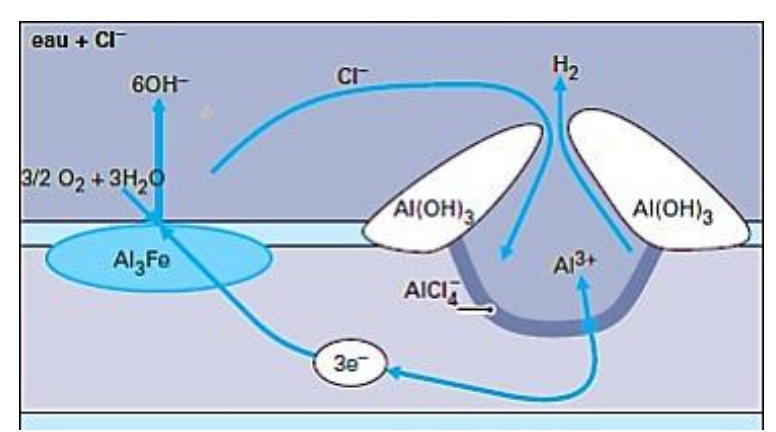


Figure 20: Evolution of the bite [27].

In this part of our work, we will start by presenting the material used and we will focus on the equipment and procedures used to carry out the experimental protocol. We will also list the characterization tools used.

VI. Materials used

The samples used in our study were taken from aluminum alloy plate that underwent hot rolling followed by cold rolling to ensure a history comparable to that of nuclear fuel cladding. The chemical composition of this alloy was analyzed using this samples are XRF equipment (see Table 6).

Table 7: Chemical composition range of Alloys 6061 (ASTM B209) [18].

alloy	Si	Fe	Cu	Mn	Mg	Cr	Zn	Ti	another
AA6061[4]	0,40- 0,80	0,70	0,15- 0,40	0,15	0,80- 1,20	0,04- 0,35	0,25	0,15	Al: solde
AA6061(our result	0.636	0.19	0,219	0.071	1.17	0.318	0,009	0,012	Al: 96.87(0.55)

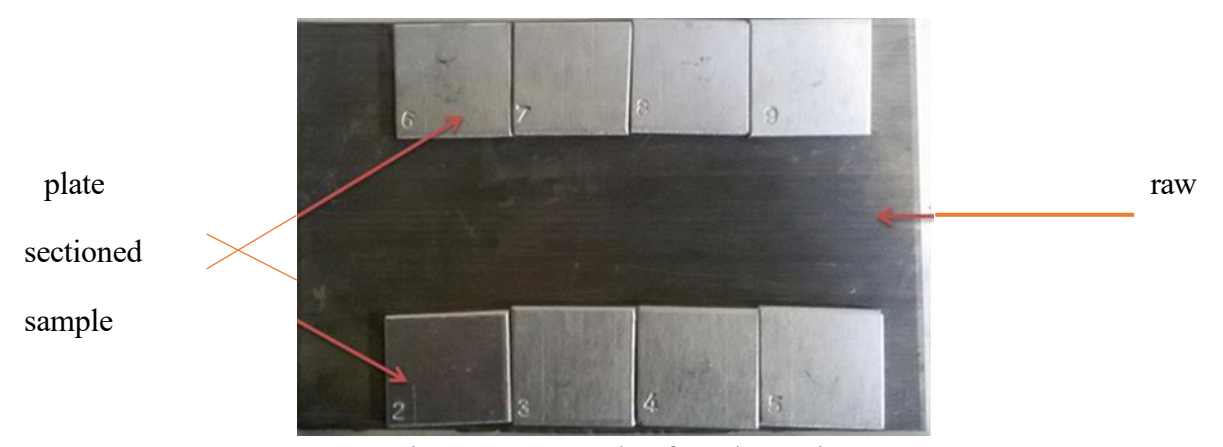


Figure 21: example of used sample

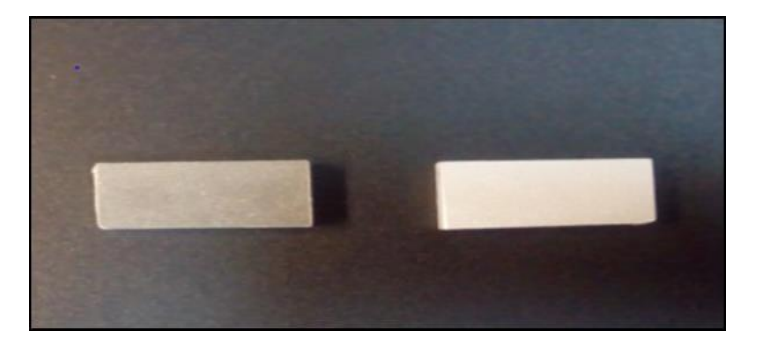


Figure 22: plates before and after pickling.

VI.1. Sample preparation

VI.1.1. Sample Cutting

The 6061 aluminum samples used in our study were cut to the following dimensions:

- 05 samples for electrochemical analysis, with a surface area of 1 cm² was prepared;
- 02 samples for SEM and XRD analyses, were cut into $3 \times 3 \times 0.5$ cm, with a 0.1 cm diameter hole for handling purposes.

Dimensional adjustments and sample cutting were performed using an automatic precision micro-saw equipped with a diamond disc, brand PRESI, model MECATOM T300 (see Figures 21 and 22). To avoid any alteration of the sample's microstructure, the cutting process was carried out cold, with a continuous flow of coolant. The dimensions of all samples were measured using a micrometer and a caliper.

VI.12. Mechanical polishing

Polishing is carried out to obtain a smooth and flat surface, allowing for accurate observation of pits under the microscope. A coarse and intermediate polishing is first performed using medium to fine grit abrasive papers (grits 240, 400, and 600). Finally, a fine polishing is carried out using finer abrasive papers (grits 800 and 2400) (figure 25), followed by a finishing step with a diamond paste suspension of 3 μ m, then 1 μ m, to achieve a mirror-like surface.



Figure 23: PRESI polisher, tech265



Figure 24: diamond paste suspension of 3 μm, then 1 μm.

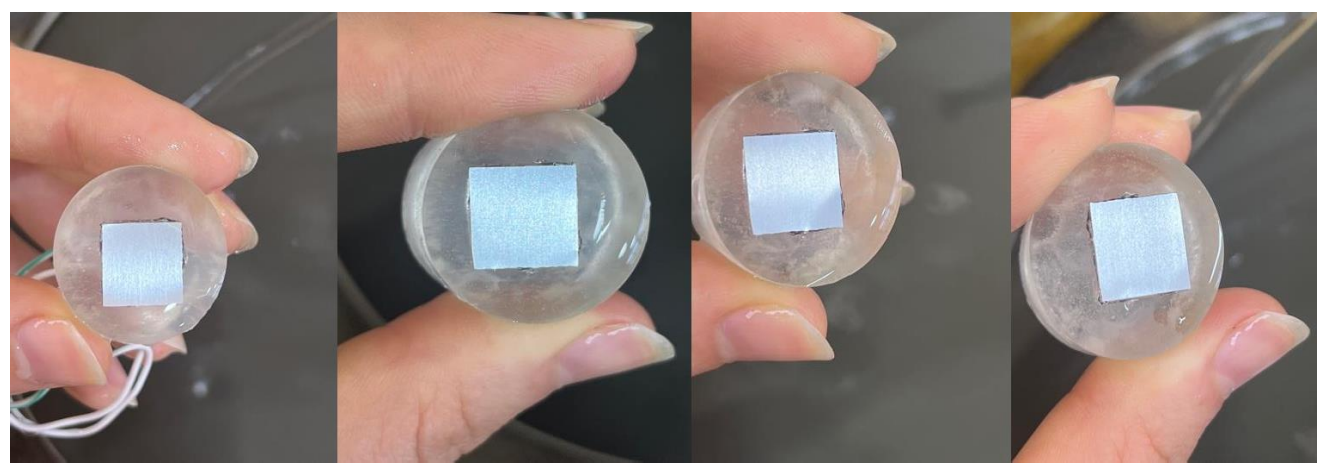


Figure 25: steps of mechanical polishing with four sandpapers (600, 800, 1200 and 2400)

VI.13. Standard pickling Procedure

The pickling procedure was carried out in order to evaluate the surface conditions. Before each pickling step, a cleaning and degreasing process must be carried out by immersion in an ultrasonic tank with neutral detergent (50% of. Acetone +50% ethanol) for 10 minutes.

VI.1.3.1. Digressing

Degreasing is an important operation before undergoing a surface treatment, in order to remove oils, greases, or other soils. It allows to change from a soiled, and generally hydrophobic, surface to a surface free of impurities, chemically and physically capable of being properly and uniformly pickled without parasitic chemical interactions. The degreasing was done using acetone and ethanol by rubbing with a clean paper towel.

VI.1.3.2. Pickling

The surface treatment process of the samples will include the following steps: (see figure 26 and 27)

- a) pickling in a sodium hydroxide solution heated to 70 °C with a concentration of 2M for a few seconds;
- b) rinses with deionized water (at room temperature);
- c) neutralization in a 60% concentration HNO₃ solution for 2 minutes;
- d) rinses with demineralized water (at room temperature) and then a second rinse with demineralized water at a high temperature;
- e) cooling and drying by a dryer.

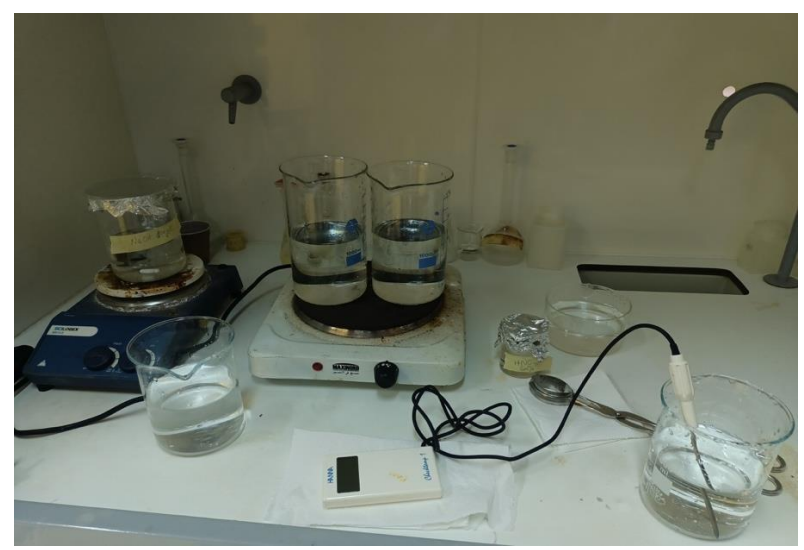


Figure 26: the procedure and steps of pickling under a chemical fume hood.

- The surface treatments applied include the following combinations:
- sample treatment (T1): Mirror Polished;
- sample treatment (NaOH) (T2): mirror polished + NaOH (80s at 70° C) + rinse H_2O (25°C);
- sample treatment (Boehmite) (T3): mirror polish + NaOH (80s at 70° C) + rinse H_2O (25°C) + HNO_3 (2mins 60%) + rinse H_2O (25°C) +rinse H_2O 70°C+ H_2O (2mins at 70°C);
- Sample treatment (Bayerite) (T4): mirror polish + NaOH (80s at 70° C) + rinse H_2O (25°C) + HNO_3 (2mins 60%) + rinse H_2O (25°C) +rinse H_2O 70°C + H_2O (2mins at 70°C);.
- Sample treatment (raw sample) (T5).

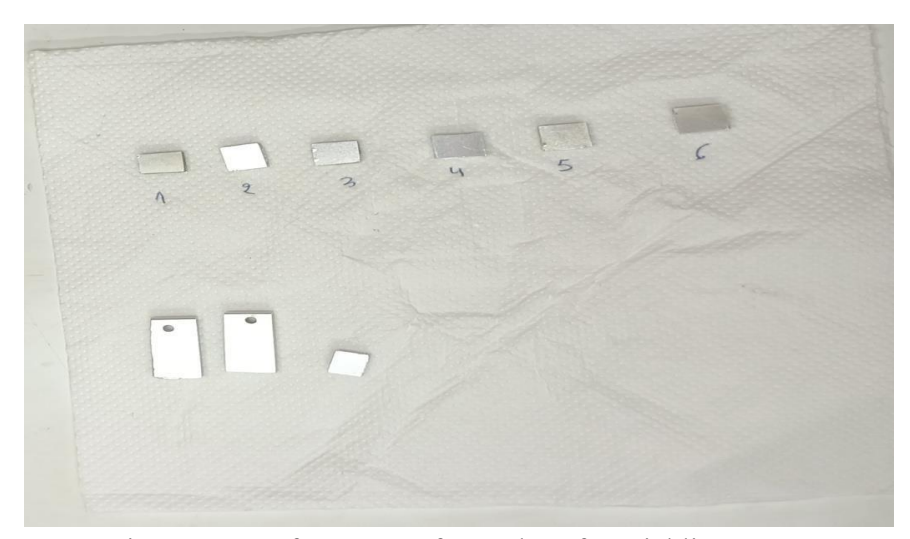


Figure 27: surface state of samples after pickling.

Following the pickling process, the samples exhibited a reduction in mass shown in table 8.

Sample mass (g)	Before pickling	After pickling
Surface treatment		
Boehmite (electrochemical)	1.1670	1.1447
Bayerite (electrochemical)	0.9489	0.9296
Boehmite (SEM)	6.1681 5.1458	6.1131 5.0984
Bayerite (SEM)	5.2930	5.2473
NaOH	1.3437	1.3173

Table 8: mass of different sample a before and after pickling

VI.14. Autoclave

The autoclave used is a vertical hydrothermal reactor, equipped with digital temperature control. It features a stainless-steel chamber with a secure, bolted lid for high pressure treatments. It was used to treat aluminum samples at controlled temperatures to promote surface layer formation.



Figure 28: vertical hydrothermal autoclave reactor used for surface treatment (boehmite T >100 °C).

- The conditions applied to samples in the autoclave for having these surface treatments include the following combinations:
- T1 treatment : Autoclave (3 days with a Temperature >100°C "Boehmite Treatment");
- T2 treatment (NaOH): autoclave (3 days with a temperature >100°C "Boehmite treatment");
- T3 treatment (Boehmite): autoclave (3 days with a temperature >100°C);
- T4 treatment (Bayerite): autoclave (3 days with a temperature <100°C bayerite treatment);
- T5 treatment (Raw sample): autoclave (3 days with a temperature >100°C "Boehmite Treatment").

Following the autoclave step, the samples exhibited a gain in mass due to the formation of hydroxides layers (Bayerite and Boehmite) shown in table 9.

Table 9: mass of different sample before and after autoclave

Sample mass(g)	Before autoclave	After autoclave	
Surface treatment			
Boehmite (electrochemical)	1.1447	1.1482	
Bayerite (electrochemical)	0.9296	0.9291	
Boehmite (SEM)	6.1131	6.1179	
Bayerite (SEM)	5.2473	5.2474	

VI.2. Characterization tools

VI21. Determination of the mass variation

In order to determine the mass loss of each sample, we use A brand analysis balance KERN model AEJ 220-4M to carry 200 grams and precision 10⁻⁴.



Figure 29: KERN analysis scale with a 200-gram range.

VI22. Measurement of conductivity

The conductivity of the water used during our experiments must be less than 2 μ S/cm. Additionally, the monitoring of conductivity during the dissolution study is carried out using a WTW Cond 3110 model conductometer.



Figure 30: conductivity meter model Cond 3110-CRND-.

VI23. Measurement of the electrical contact

To check the electrical continuity of the sample surface, a digital multimeter of type A830L is used.



Figure 31: digital multimeter

VI.3. Used Equipment:

VI31. Ultrasonic bath:

Cleaning and degreasing step must be carried out by immersion in an ultrasonic tank DAITHAN Scientific (figure 32) with neutral detergent (50% of. Acetone +50% ethanol) for 10 minutes.



Figure 32:(a) ultrasonic tank, (b) Acetone and ethanol for degreasing.

VI32. Temperature Control

In order to perform the temperature variations of the NaOH solution, as well as the heating of the rinse water to 70°C, we use a magnetic heating plate agitator that allows the samples to be homogenized and heated simultaneously. The agitator is of the Scilogex brand and model MS-H-S (shown in figure 34) with a maximum capacity of 340 °C and 1500 rpm. Temperature control is done using several portable digital thermometers from HANNA and Checktemp1 models .



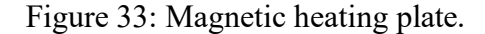




Figure 34: Hand-held digital thermometer.

VI33. Preparation of solutions

VI.3.3.1. Neutralization solutions

The nitric acid-based neutralization solution used is at 60% concentration, and has been prepared from a stock solution of 69% HNO_3 . Demineralized water (always around 2 μ S/cm) was used for dilution to avoid undesirable interactions.



Figure 35: Preparation of the neutralization solution.

VI.3.3.2. Pickling solutions:

The solutions of NaOH at different concentrations are Developed has been prepared from different quantities of caustic soda crystals, solubilized in demineralized water (still around 2 μ S/cm). The soda crystals are brand SIGMA-ALDRICH High Purity (99.6 % at a minimum).



Figure 36: SIGMA-ALDRICH caustic soda crystallites.

VI.4. Characterizations techniques

The purpose of this section is to explain the general principles of the various characterization techniques. These techniques can be divided into three groups:

- Microscope optic;
- The Scanning Electron Microscope (SEM);
- X-ray Diffraction (XRD);
- electrochemical and corrosion resistance: (OCP and poteniodynamic polarization).

VI4.1. Optical microscope:

The surface morphology of the samples (As-received, Polished, pickled (chemically cleaned), Pickled (or chemically cleaned), Electrochemically corroded) was characterized using a metallographic microscope manufactured by ZEISS figure 37). morphology pictures were taken by the Axio Vision Rel 4.6.3 image analysis software.



Figure 37: Optical microscope ZEISS-CRND-.

VI42 The Scanning Electron Microscope (SEM):

SEM used is the Philips XL30-FEG type, available in the spectroscopy department of the nuclear research center in Algiers. It is an environmental scanning electron microscope equipped with a field emission gun, allowing for a resolution of 2 nm in observation. It primarily allows for the characterization of microstructures present in a material through surface observation. The information provided by this technique concerns the state of the observed microstructures, namely:

- The morphology;
- The dimensions:
- The distribution:

Equipped with an X-ray microanalyzer, it constitutes a localized method of chemical characterization, namely:

- Determination of the local chemical composition
- Determination of the distribution of defined elements along a line (Concentration profile)
- Highlighting the distribution of defined elements across a surface (Mapping)

 The environmental mode that the microscope possesses allows for the characterization of matter in its natural state using a controlled gas atmosphere:
- The hydrated samples
- The non-electrically and thermally conductive samples



Figure 38: Scanning Electron Microscope XL30-FEG -CRND-.

VI43. X-ray Diffraction (XRD):

X-ray diffraction is an analytical technique that allows us to obtain information about the crystalline properties of a material, such as the lattice parameter and the interplanar distance. A crystal can be seen as the three-dimensional periodic repetition of elements (atoms or molecules), called nodes, marked by black discs in Figure 39 The diagram represents a cross-section of lattice planes passing through the centers of these elements, spaced by a distance "d". The angle θ (Bragg angle) determines the incidence of a parallel beam of X-rays on these lattice planes. Note that θ is the complement of the

usual incidence angle in optics. The optical path difference between the two specific light rays represented is:

$$AC + CB = 2 d \sin \theta \dots VI.4.3.1$$

They interfere constructively when the path difference is equal to an integer p of wavelength. This is Bragg's law:

2d hkl sin
$$\theta$$
=n λ VI.4.3.2

Where:

d hkl: The interplanar distance

 θ : The half-angle of deviation;

n: The order of reflection;

 λ : The wavelength of X-rays.

X-ray diffraction analyses were performed using a PHILIPS model D5000 device, with a voltage of 45kV and a current of 40 mA. The X-rays were emitted from a lamp equipped with a copper anode, whose main line had a wavelength of 0.154060 Å. The scanning speed was 0.02 (2-Theta) degrees per minute and the analyzed range was from 10 to 120 degrees (2-Theta).

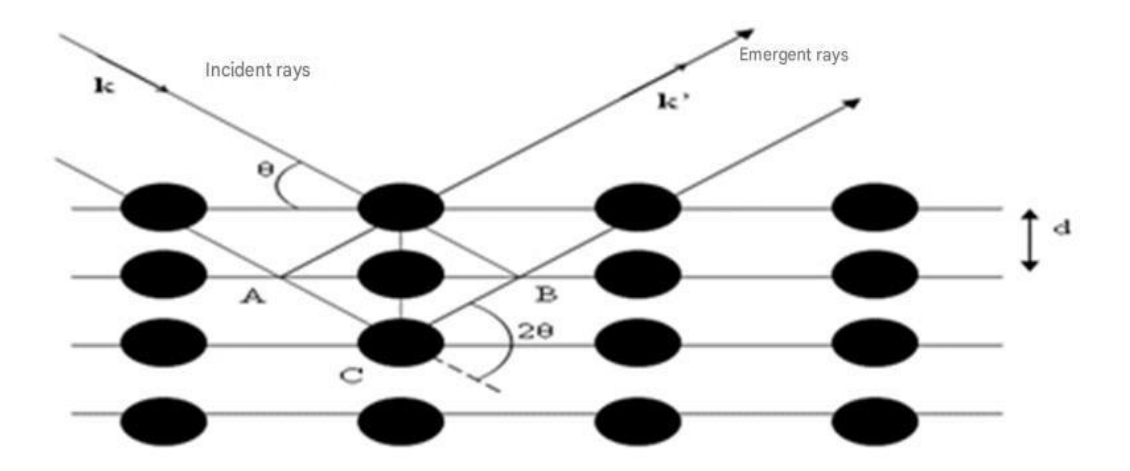


Figure 39: Reflection of X-rays by a family of lattice planes spaced a distance d apart.

VI44. Electrochemical characterization:

VI.4.4.1. Experimental dispositive:

The electrochemical experiments were carried out in a cylindrical Pyrex glass cell with a capacity of 500 ml. This cell contains three electrodes (figure 40), and the electrode setup consists of two electrical measurement circuits (see figure 41):

- the first circuit is used to measure the potential of the working electrode relative to the reference electrode;
- the second circuit is used to measure the current intensity between the working electrode and the counter electrode.

Working electrode: a sample of aluminum alloy Al 6061T6 with a surface area of 1×1 cm²

is immersed in the solution.

Reference electrode (Ag/AgCl type saturated with KCl): this electrode has a specific and constant potential, which allows a precisely defined potential to be applied to the working electrode.

Counter electrode: a platinum electrode used to determine the current flowing through the working electrode during potentiodynamic scans.



Figure 40: showing the Counter electrode, Reference electrode

The electrodes of the cell are connected to a VOLTALAB PGZ301 potentiostatgalvanostat, controlled by a microcomputer (Voltameter software), which enables experiment monitoring, curve visualization, and automatic data recording, as shown in





Figure 41: photography of assembly experimental

III.1.1.1. Electrochemical Behavior Study

III.1.1.1. Electrochemical behavior of aluminum

The electrochemical behavior of aluminum is largely influenced by its natural oxide film, which plays a key role in the metal's corrosion resistance. The potential measured on aluminum is not that of the bare metal itself, but rather a mixed potential resulting from

both the oxide layer and the underlying metal. It is impossible to measure the true potential of the metal alone because the oxide film forms almost instantaneously in oxidizing environments even in water within a fraction of a second, or even a thousandth of a second. In environments that are nearly neutral in pH, corrosion on aluminum typically occurs in the form of localized pits[27].

VI.4.4.1.1. Open Circuit Potential (OCP) Measurement

This technique allows monitoring the evolution of the potential as a function of time (E = f(t)) when no current is flowing to the working electrode. It is used to determine the phenomenon occurring on the electrode surface (corrosion, passivation, or both).

VI.4.4.1.2. Potentiodynamic Polarization

Potentiodynamic polarization is a steady-state electrochemical technique that involves applying a potential E to the working electrode and measuring its current response. The potential sweep produces the polarization curve I = f(E).

Plotting this curve allows for the calculation of parameters such as corrosion current (I_{corr}), corrosion potential (E_{corr}), corrosion rate (V_{corr}), and polarization resistance.

The tests were carried out with a scan rate of $V = 10 \text{ mV} \cdot \text{s}^{-1}$, and the considered potential range was from -1000 mV vs to +1000 mV vs. E_{corr} (a potential sweep from the cathodic domain to the anodic domain).

VI.4.4.2. Preparation of electrolyte

The electrolyte used for nitrate reduction is a 0.05 M NaCl solution.

- 500 mL of distilled water; all the solutions studied are prepared just before the experiment;
- 1.461 g of NaCl crystals.

It is also necessary that, before preparation, all glassware is carefully cleaned and thoroughly rinsed with distilled water.



Figure 42: materials used for the preparation of 0.05M NaCl electrolyte (distilled water, chloride sodium and a magnetic agitator)

o reference electrode saturation with KCl crystallites:



Figure 43: KCl crystallites.

VI.4.4.5. Samples preparations

After oxidation in the autoclave, the samples are mounted with a cold-curing epoxy resin to isolate all surfaces except the analytical surface exposed to the NaCl solution. Electrical contact between the sample and the potentiostat is ensured using a copper wire securely attached to the sample before mounting. This preparation ensures reliable electrochemical measurement. (See figure 44) for an illustration of the mounting.



Figure 44: Assembly Preparation of samples for electrochemical tests

Before presenting the results of the study on the electrochemical behavior in a mildly chlorinated environment, we considered it useful to begin this chapter with the characterization of the material under study, namely the aluminum alloy 6061.

VII. 1. Observations under the optical microscope

VII.1.1 Characterization of the surface condition of the samples

The optical micrographs in (Figures 45) illustrate the surface condition of the AA6061 alloy with (a) and without (b) prior polishing. These observations show that the surface condition of figure (b) exhibits scratches and dirt due to the rolling of the plate, whereas for figure (a) it is clear that the surface is clean and uniform. Therefore, the polished surface shown in (Figure 45) (a) was selected as the reference surface for all subsequent experiments in this study

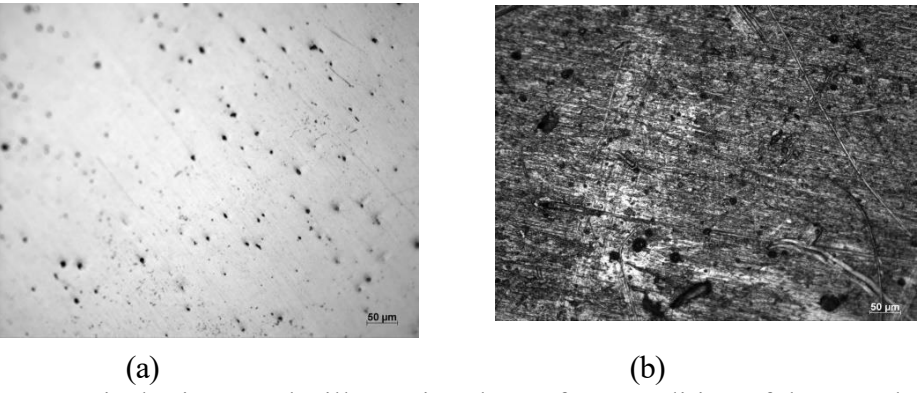


Figure 45: Optical micrographs illustrating the surface condition of the samples: (a) mirror-polished, (b) rough state.

VII.1.2 After pickling and oxidizing:

In Figure 46. (b): representing the sample after pickling, the surface appears relatively clean but exhibits numerous circular and elongated grooves. These features are characteristic of the selective dissolution of surface oxides and intermetallic phases such as Mg_2Si or Al-Fe-Si compounds during the acidic pickling process. The surface roughness and visible etching traces indicate enhanced surface reactivity, which facilitates better adhesion in subsequent surface treatments.

Figure 46. (c): shows a darker, more homogeneously textured surface, corresponding to the sample after autoclave surface treatment. The dense distribution of dark rounded particles across the surface suggests the formation of a fine hydroxide layer, most likely composed of Boehmite (AlOOH) and possibly Bayerite (Al(OH)₃), as confirmed later by XRD analysis. The uniformity of the layer and its adherence to the substrate indicate successful hydroxide

growth and good surface coverage, although the substrate remains partially visible, suggesting a thin film.

The morphological differences between the two figures clearly highlight the effect of chemical treatment on the alloy surface. The treatment not only modifies the topography but also contributes to the formation of a protective hydroxide film that plays a key role in enhancing the corrosion resistance of the material in saline environments.

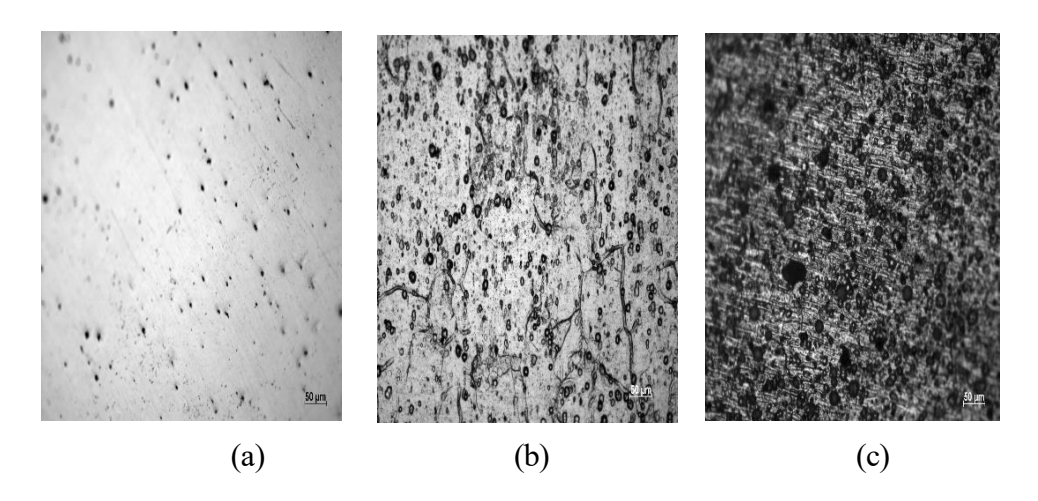


Figure 46: Optical micrographs showing the surface condition of the samples (a) polished, (b) pickled, (c) oxidized.

VII.2 X-ray diffraction analysis (XRD):

The technique used for identifying solid phases is X-ray diffraction (XRD). XRD analyses in 2θ mode were performed on AA6061 samples oxidized at different temperatures (70°C and 100°C) for 3 days. This technique is intended to reveal all the phases present in the samples.

- AA6061-70 °C
- AA6061-100 °C

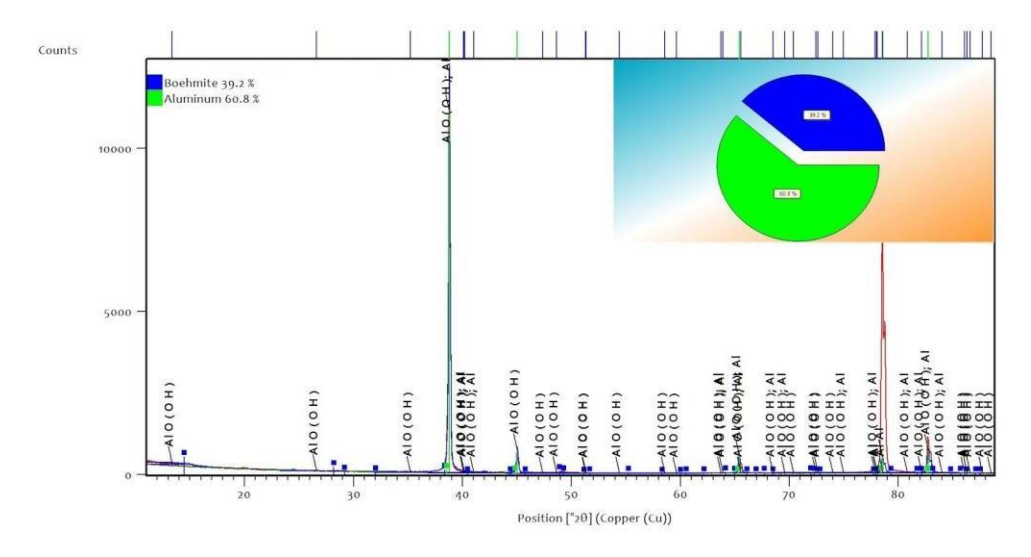


Figure 47: XRD pattern of the corrosion product obtained at 100°C for 3 days

In the X-ray diffraction pattern shown in (Figure 47) two crystalline phases can be observed, Boehmite and metallic aluminum.

- Boehmite (AlOOH): ~39.2% (in blue on the pie chart). is identified by its characteristic peaks around $2\theta \approx 14$ –15°, 28–29°, 38–40°, and 48–50° The intense peaks at $2\theta \approx 38^\circ$, $\approx 44^\circ$, $\approx 65^\circ$ and $\approx 78^\circ$ correspond to the (111), (200), (220) and (311) planes of metallic aluminum, consistent with Al-centered cubic lattice diffraction.
- ➤ Metallic Aluminum (Al): ~60.8% (in green).

These proportions are characteristic for a thin boehmite layer formed on a bulk aluminum substrate, where most of the XRD signal originates from the underlying aluminum. The coexistence of boehmite and aluminum peaks indicates that the surface is partially covered by a crystalline layer which remains adherent but not thick enough to fully cover the substrate. This result supports the hypothesis that the hydrothermal treatment successfully produced a thin, protective layer without significantly altering the metallic base.

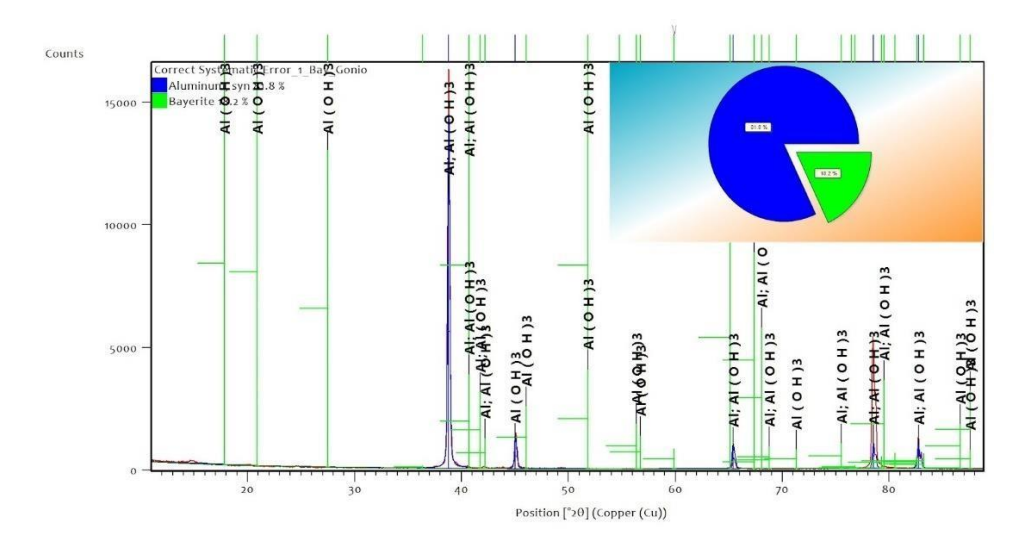


Figure 48: XRD diagram of the corrosion product obtained at 70°C for 03 days

The X-ray diffraction (XRD) pattern shown in (Figure 48) shows distinct diffraction peaks corresponding to metallic aluminum (AA6061 alloy, face-centered cubic structure), typically located around $2\theta \approx 38^{\circ}$, 44°, and 65°, which correspond to the (111), (200), and (220) crystallographic planes, respectively. Additional peaks observed at approximately $2\theta \approx 19.2^{\circ}$, 20.5° , and 40.8° are attributed to bayerite (α -Al (OH)₃). The simultaneous presence of aluminum and bayerite peaks confirms the coexistence of two phases: the metallic substrate (approximately 81.8 %) and a hydroxide layer composed of bayerite (approximately 18.2 %).

This hydroxide layer is likely formed as a thin nanocrystalline or microcrystalline bayerite film deposited on the metal surface, but is probably not fully continuous. The relatively low content of bayerite (~18.2 %) suggests that the hydroxide layer is thin or discontinuous. In practice, this means that the Al (OH)₃ film does not completely cover the metal surface and is limited to a superficial deposit. Such a partial film therefore provides limited effectiveness as a protective barrier against corrosion.

VII.3. Observations using a scanning electron microscope (SEM)

VII.3.1 Boehmite layer

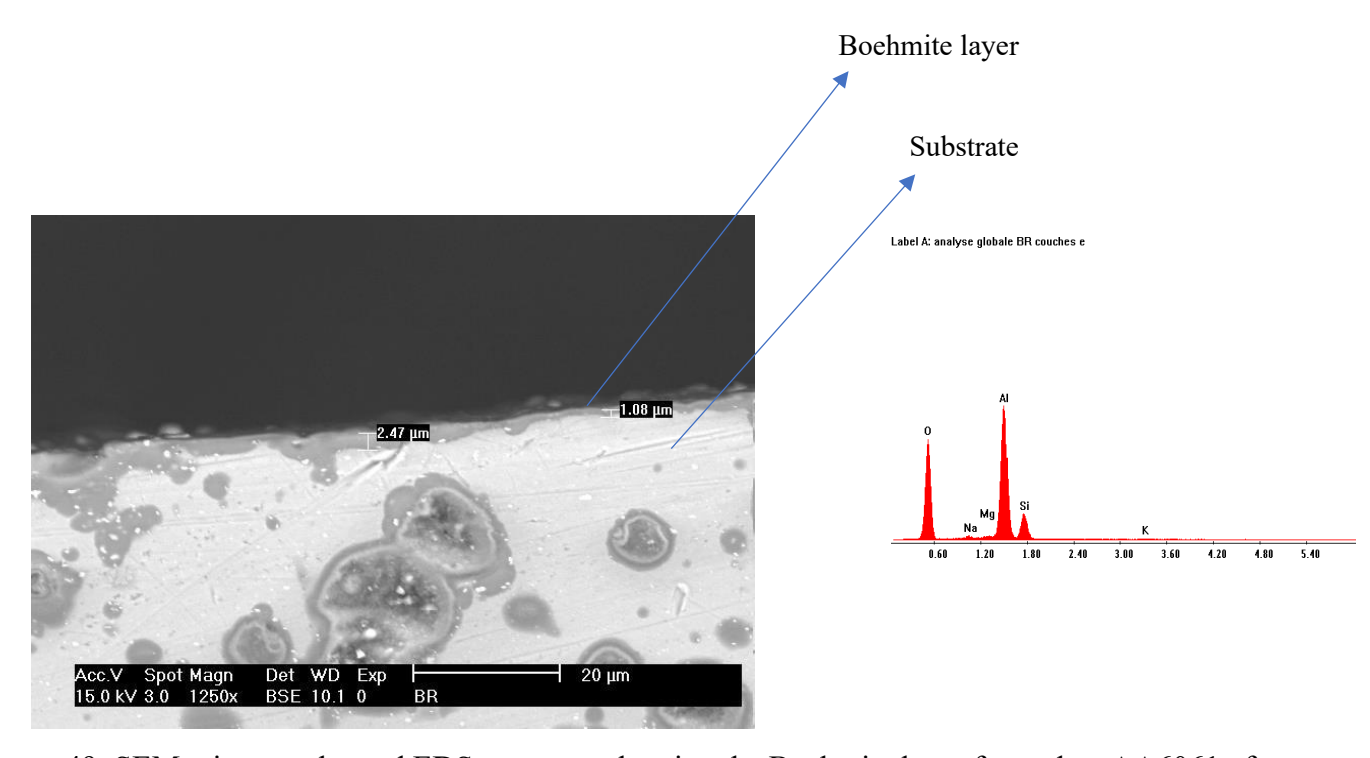


Figure 49: SEM micrography and EDS spectrum showing the Boehmite layer formed on AA6061 after autoclave treatment

Table 10: Elemental composition (%) of Boehmite

Elem	Wt %	At %
OK	46.45	59.59
NaK	0.97	0.87
MgK	0.81	0.69
AIK	39.73	30.22
SiK	11.24	8.21
KK	0.79	0.41
Total	100.00	100.00

According to cross-sectional scanning electron microscope (SEM) analysis, a compact, continuous surface layer formed on the 6061-aluminum substrate as a result of the autoclave treatment. The thickness of this surface layer varies by testing (1.08 µm - 2.47 μm), indicating the successful formation of a thin protective layer. EDS analysis confirmed a high aluminum (39.73 wt%) content accompanied by a significant oxygen signal (46.45 wt%) (see table 9), suggesting the formation of an aluminum oxyhydroxide layer, specifically boehmite. Besides the homogeneous oxide layer, traces of sodium, magnesium, and silicon could be attributed to the alloy base composition either to residues from the treatment bath (NaOH). While looking at the SEM image, we observe crosssection clusters of hydroxides which have varying dimensions likely from localized accelerated corrosion microstructural variations of the aluminum alloy morphology. The high intensity of the aluminum peak confirms that the aluminum remains the dominant element in the analyzed zone, meaning the layer is not thick enough completely to mask the substrate. These results confirm that the surface treatment allowed the formation of a thin, adherent, and potentially protective layer without significantly changing the surface chemistry of the base metal.

The presence of silicon (11.24% by weight) is notable. In the AA6061 alloy, Si originates primarily from Mg_2Si precipitates and other Si-rich phases inherent to the alloy's microstructure. During the hydrothermal treatment, a portion of this silicon can migrate toward the surface or become incorporated within the hydroxide layer. This behavior is typical for AlMgSi alloys.

The detection of minor amounts of Na (0.97%), Mg (0.81%), and K (0.79%) can be attributed either to residues from the hydrothermal solution depending on the purity of the water used or to trace elements originating from the alloy itself. For example, Mg is commonly present

VII.3.2. Bayerite layer

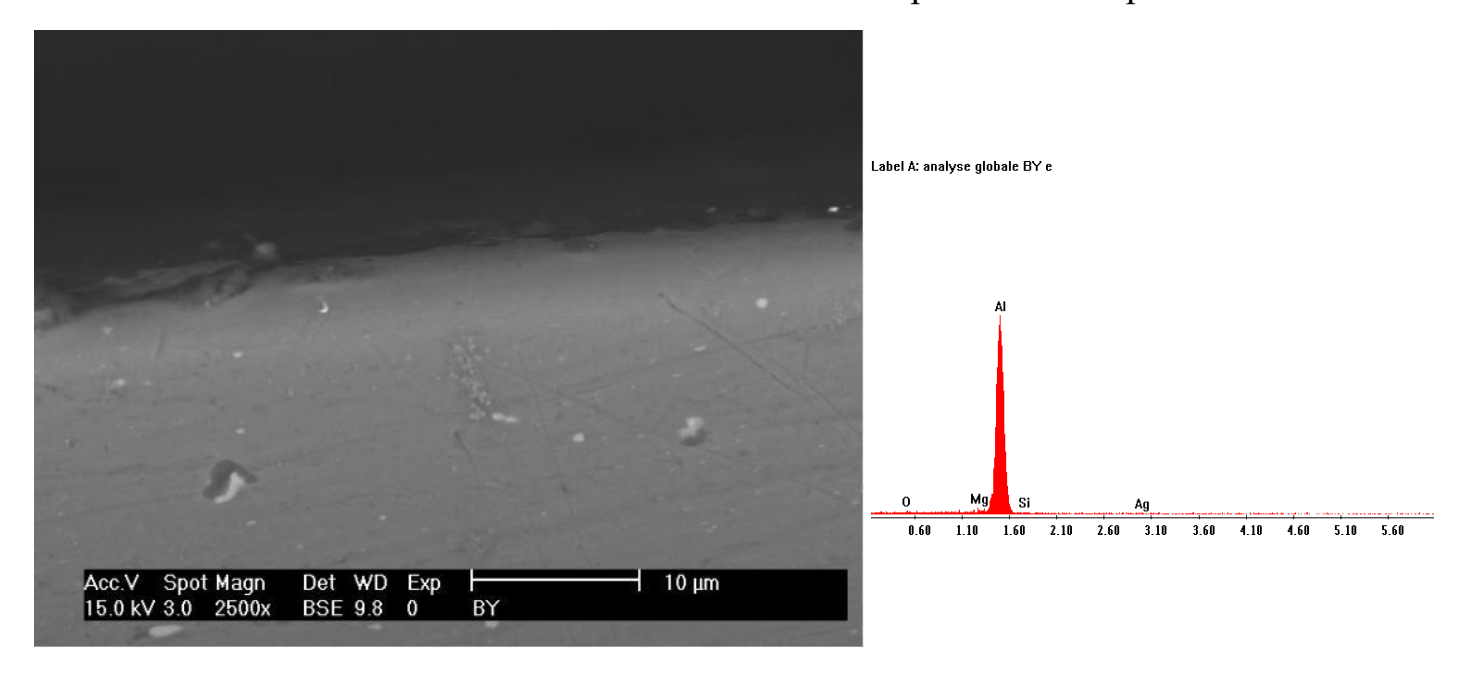


Figure 50: SEM image and EDS spectrum showing the Bayerite layer formed on AA6061 after autoclave treatment

Table 11:Elemental composition (%) of Boehmite

Elem	Wt %	At %
ок	0.54	0.91
MgK	0.78	0.86
AlK	98.68	98.24
SiK	0.00	0.00
AgL	0.00	0.00
Total	100.00	100.00

Through the scanning electron microscopy (SEM) image of the sample that underwent thermal treatment in the autoclave under conditions aimed at forming a Bayerite layer.

The surface microstructure appeared nearly identical to that of the untreated substrate, this indicate that the formed layer appeared non uniform, irregular or incomplete surface coverage. This observation was further confirmed by energy dispersive X ray spectroscopy analysis, which revealed a very high aluminum content (approximately 98.68% by weight) and a very low oxygen content (around 0.54% by weight) (see table 11). These results suggest that, due to the extremely low thickness of the oxide layer, it could not be clearly detected by SEM imaging (≤10nm)[50].

The thermal treatment was conducted at a relatively low temperature (below 90°C), with the pH maintained around 6 close to neutral. under such condition hydroxide ions (O H^-), which are essential for the formation of $Al(OH)_3$ are scarce. Therefore, the reaction conditions were insufficient to promote the development of detectable Bayerite layer [51].

VII.4. Electrochemical results

VII.4.1 Open Circuit Potential (OCP) results

Open Circuit Potential Monitoring (OCP), the Figure 51 shows the (OCP) variation versus time diagrams for untreated and treated aluminum alloys in 0.05 M NaCl at 25 °C.

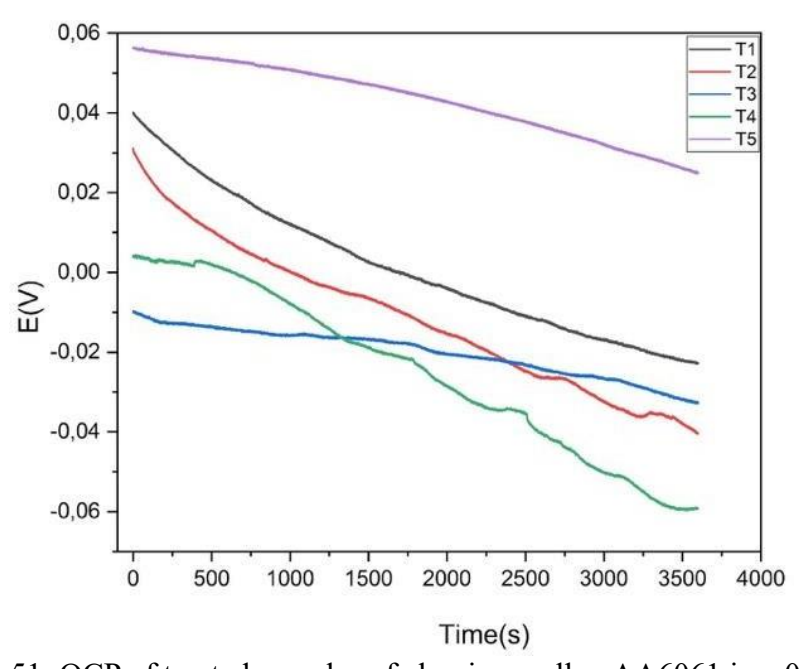


Figure 51: OCP of treated samples of aluminum alloy AA6061 in a 0.05M NaCl

After the initial drop observed at the beginning of immersion, the OCP curve of the T5-treated sample gradually decreases and then stabilizes around 0.035 V (showing a potential difference of 0.02 V in the last 20 minutes), until the end of the relative stabilization period, which lasts approximately 1 hour.

The OCP curves show different initial potential values, as each one represents the electrochemical response of a sample in NaCl solution. These variations arise from the

distinct surface treatments applied whether through pickling or the formation of oxide layers like bayerite or boehmite which influence the initial surface reactivity.

- T1 starts with 0.04 V;
- T2 starts with 0.03 V;
- T3 starts with -0.01 V;
- T4 starts with 0.005 V;
- T5 starts with 0.06 V.

With an average potential difference (in the last 20 minutes of the OCP curves) of 0.017 Volts, this phenomenon showed remarkable stability during the last 20 minutes of these tests, which allowed us to move on to the production of the polarization curves.

VII.4.2 Polarization curves

The polarization curve of the interface (metal/solution) is a fundamental characteristic of electrochemical kinetics. The shape of the Tafel lines provides information on the surface activity of the aluminum alloy AA6061, the corresponding charge transfer reactions, and the reaction mechanism deduced from the anodic and cathodic slopes [52,53]. The polarization curves for aluminum alloys without treatment and with treatment in 0.05 M NaCl at 25 °C are shown in figure 52. The shape of the polarization curves indicates on the one hand a decrease in the corrosion current density in the case of the treated samples compared to the raw sample, so in this case we have an improvement in corrosion resistance. This result is due to the layers that we formed during this study, the formation of which was previously confirmed by metallographic characterization (SEM, XRD)

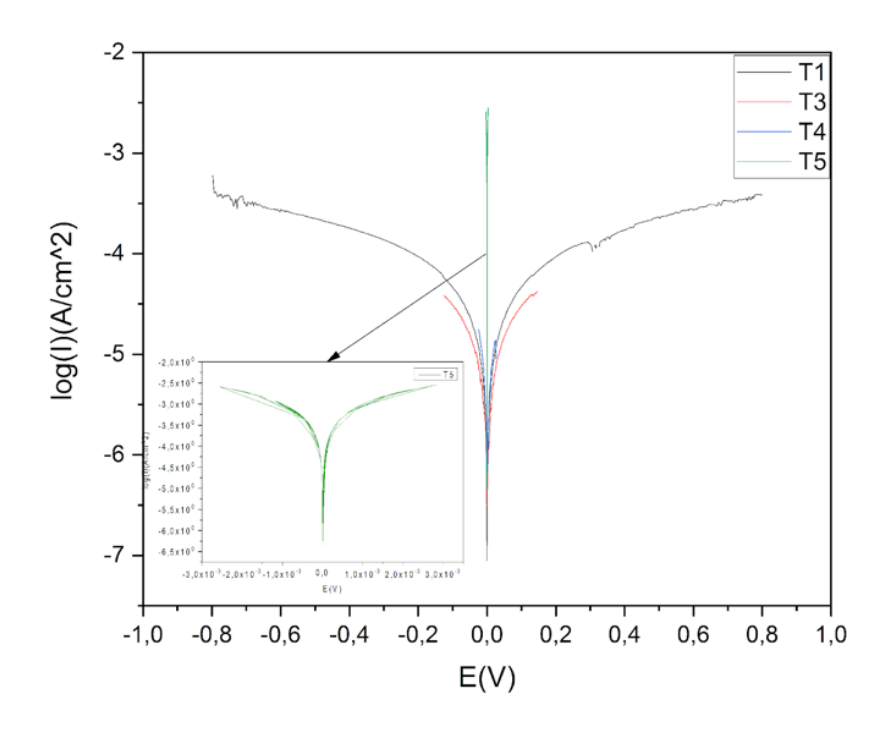


Figure 52: polarization curves of treated samples of aluminum alloy AA6061 in a 0.05M NaCl

VII.4.2.1 Comparison of Protective Layer Performance

The electrochemical parameters derived from the polarization curves of the different samples, such as the stabilization potential (E_0) , corrosion current density (I_{corr}) , polarization resistance (R_p) are compiled in Table 12.

Table 12: the results of polarization (Tafel tests) of treated samples of AA6061 alloy

Treated sample	Т3	T4	Т2	T1	T5
Corrosion parameters					
E0 (v)	-0.033	-0.06	-0.04	-0.02	0.035
Ic $(\mu A * cm^{-2})$	9.69	29.85		11.92	97.39
Rp (<i>Ohm. cm</i> ²)	3420	1460		2400	402.8

• T3

Boehmite showed the highest corrosion resistance: It exhibited the lowest corrosion current density ($I_{corr} = 9.69 \mu A/cm^2$), which means the corrosion rate has been reduced drastically. The highest polarization resistance (Rp=3.42 $k\Omega$. cm^2) was registered, which is the result of the formation of a protective surface layer. These results indicate that the Boehmite layer was formed effectively and acted as a barrier, thus preventing the diffusion of ions and water to the underlying metal, the corrosion mechanisms were very much reduced.

T1

The sample treated only with thermal autoclaving showed moderate improvement in corrosion resistance. It registered a corrosion current density of $(I_{corr}=11.92\mu A/cm^2)$ and a polarization resistance of (Rp=2.40 $k\Omega$. cm^2). These values indicate that an irregular or weakly adherent hydroxide film was probably formed on the surface due to residual surface contamination and insufficient cleaning and chemical conditions to, promote effective oxidation process. Compared to the boehmite-treated sample, the H-treated sample exhibits lower adhesion of the protective layer. This behavior can be attributed to the pickling treatment, which induces a rougher surface state, thereby enhancing the adhesion of the thin boehmite layer and improving its corrosion resistance, as reflected in the polarization curves.

• T4

The sample intended for the formation of Bayerite demonstrates significantly poorer corrosion resistance. The sample was characterized by a higher (Rp=29.85 $k\Omega$. cm^2) value and a lower ($I_{corr} = 1.46 \mu A/cm^2$) one than the Boehmite and H treated ones. This is a typical situation when a surface layer is not fully formed or is irregular, which correspond to the SEM and EDS data, where the oxygen concentration was extremely low.

• T5

It recorded the highest ($I_{corr} = 97.39$. $\mu A/cm^2$), which means a high corrosion rate. The lowest (Rp=402 Ω . cm^2) is the absence of any barrier of protection of the sample. These results are a clear indication of the necessity of surface treatment in a big way for the AA6061 alloy to show improved corrosion resistance.

• T2

polarization curves representing the metal electrolyte interaction do not appear when Onley NaOH is used in the surface preparation stage. The cause of this phenomenon can be a "smut" layer that is made up of insoluble oxides of additional elements (such as magnesium and silicon). Such a layer cuts off the reaction of oxidation and does not allow a regular hydroxide layer to be formed during the surface treatment. According, it is generally advised to carry out an acid pickling step after NaOH treatment in order to get rid of such residues and be sure that surface is clean and uniform.

VII.4.3 Observations under the optical microscope

The figure 53 shows an observation of the three samples (raw, Boehmite and Bayerite samples) after the electrochemical characterization under the optical microscope.

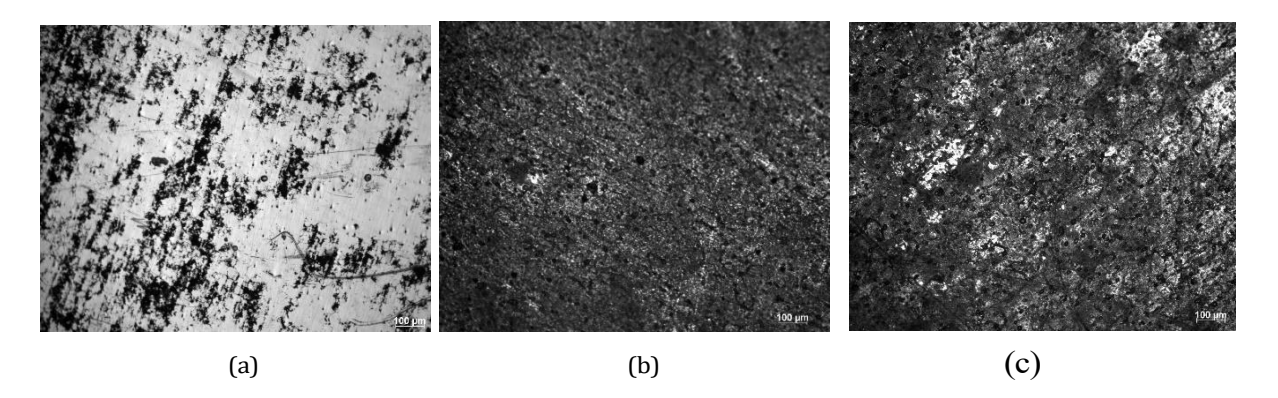


Figure 53: Optical micrographs showing the surface of the samples (a) T5, (b) T3, (c) T4.

The microscopic image of the raw sample after NaCl testing reveals a typical uniform corrosion. This is characterized by widespread surface degradation with the roughened appearance, the surface looks like it was corroded in an even way, suggesting the absence of a protective layer to shield the alloy from the aggressive chloride ion. Such a line of thought is also in line with the electrochemical data, which indicate that the sample is of weak corrosion resistance, and the absence of surface treatment is the cause thereof.

A uniform protective boehmite layer was observed, except in the very small specific attacked area, which resulted from defective or incomplete boehmite formation, The bayerite layer shows poor uniformity, which led to more pronounced NaCl-induced corrosion in certain large regions, unlike the boehmite layer. This non-uniformity explains the attacks observed in these specific areas.

Conclusion

The data clearly show that the Boehmite layer provides the best corrosion protection among the studied treatments. This is followed by the H treated sample. On the other hand, the conditions used for Bayerite formation were insufficient to form a stable protective layer

General Conclusion

The goal of this study was to improve the corrosion resistance of AA6061 aluminum alloy, which is commonly used as cladding in research reactors. Since this material operates in humid and aggressive environments, especially in the presence of chloride ions, protecting its surface is crucial to ensure its long-term performance and safety.

To achieve this, we investigated various surface treatments, particularly **Boehmite** and **Bayerite**, that are intended to create protective oxide or hydroxide layers. In order to create a more reactive surface that can better support the formation of oxide layers, we first prepared the surface by pickling, which helped remove natural oxides and surface contaminants.

Results from the **surface treatment in the autoclave** were encouraging, particularly when the temperature was higher than 100 °C. We were able to create a Boehmite layer in these circumstances, and it looked uniform, compact, and firmly adhered to the substrate. While EDS analysis verified a high oxygen content, suggesting the formation of aluminum oxyhydroxide, SEM cross-sectional analysis revealed a layer thickness ranging from 1.08 to $2.47~\mu m$. Additionally, **crystalline Boehmite** covering a sizable area of the surface was confirmed by XRD results.

On the other hand, The **Bayerite** layer, on the other hand, which developed at lower temperatures, was far less successful. Very little oxygen was found in the EDS results, and there was hardly any surface change visible in the SEM.

XRD analysis confirmed that the layer was thin and not well developed. This non-uniformity was reflected in the poor corrosion resistance seen during electrochemical tests.

The electrochemical tests, including open circuit potential (OCP) and polarization curves, clearly showed that the Boehmite-treated sample had the best corrosion performance. It had the lowest corrosion current density and the highest polarization resistance, confirming the effectiveness of the Boehmite layer as a barrier to corrosive ions. On the other hand, untreated or poorly treated samples—especially the one without any pickling—showed high corrosion rates and poor resistance.

Finally, **optical microscope observations after corrosion testing** supported these findings. The untreated sample showed signs of uniform corrosion across the surface, while the Boehmite-treated sample was mostly protected, with only a few small localized corrosion spots. The Bayerite-treated sample, however, showed larger and more irregular corrosion zones, confirming that the layer was thin and incomplete.

In conclusion, this work unequivocally shows that the formation of a Boehmite layer under carefully regulated autoclave conditions greatly increases the AA6061 alloy's resistance to corrosion. The Boehmite surface with the whole pickling treated process (T3) provided the best protection out of all the treatments that were tested. The significance of

appropriate surface preparation and treatment parameters is underscored by these findings. Future research could examine treatment optimization, long-term performance, and even combining different surface protection techniques for improved outcomes.

References

- [1] J.R. Davis, "Aluminum and Aluminum Alloys", ASM International, Ohio, (1993).
- [2] V.S. Zolotorevsky, N.A. Belovn, M.V. Glazoff, "Casting Aluminum Alloys", Elsevier, Amsterdam, (2007).
- [3] S. Joshi, W.G. Fahrenholtz, M.J. O'Keefe, "Effect of alkaline cleaning and activation on aluminum alloy 7075-T6", Appl. Surf. Sci. 257 (2011) 1859–1863.
- [4] O. Gharbi, N. Birbilis, K. Ogle, "In-situ monitoring of alloy dissolution and residual film formation during the pretreatment of Al-alloy AA2024-T3",
- J. Electrochem. Soc. 163 (2016) C240-C251.
- [5] P. Campestrini, E.P.M. van Westing, J.H.W. de Wit," Influence of surface preparation on performance of chromate conversion coatings on Alclad 2024 aluminium alloy part I: nucleation and growth", Electrochim. Acta 46 (2001) 2553–2571.
- [6]. A.Lynch ." Nuclear in decarbonized power systems with renewable energy: Flexibility assessment, modeling framework, and role in the French and Western European electric transition", Doctoral dissertation, Université Paris-Saclay, (2022).
- [7].R. L.Murray, & K. E.Holbert. "Nuclear energy: An introduction to the concepts, systems, and applications of nuclear processes". Elsevier, (2014).
- [8].J.Couturier, H. Abou Yéhia, & E. Grolleau. "Éléments de sûreté nucléaire: Les réacteurs de recherche" (pp7-12). EDP sciences, (2019).
- [9].F.H.Martens. "Research Reactors". US Atomic Energy Commission, Division of Technical Information, (1967).
- [10].M.Azzoune, L.Mammou, M. H. Boulheouchat, T.Zidi, M. Y. Mokeddem, S.Belaid, ... & A. Boumedien. "NUR research reactor safety analysis study for long time natural convection (NC) operation mode". Nuclear Engineering and Design, 240(4), 823-831, (2010),.
- [11].A.Hammoud, B. Meftah, M. Azzoune, L. Radji, B.Zouhire, & M.Amina. "Thermal-hydraulic behavior of the NUR nuclear research reactor during a fast loss of flow transient". Journal of Nuclear Science and Technology ,51(9), 1154-1160, (2010), [12].M.Durazzo, & H. G Riella. "Procedures for manufacturing nuclear research
- & H. G Riella. "Procedures for manufacturing nuclear research reactor fuel elements". LAP LAMBERT Academic Publishing, (2015).
- [13]. M.IFIRES. "Etude de comportement électrochimique de

- l'alliage AA6061 dans le milieu NaCl en présence d'inhibiteur de corrosion'. Mémoire de Magister, université Saad Dahleb De Blida, (2012).
- [14]C, Vargel, "Propriété générale de l'aluminium et ses alliages",(1999).
- [15] Lemaignan, C. "Science des matériaux pour le nucléaire". Les Ulis: EDP Sciences, (2004).
- [16]C, Vargel, "Corrosion de l'aluminium". Dunod, (1999).
- [17] Alfrey, A. C. Aluminum. Advances in clinical chemistry, 23, 69-91, (1983).
- [18] ASTM International. ASTM B209/B209M-01: Standard specification for aluminum and aluminum-alloy sheet and plat,(2002).
- [19] J. R. Davis, (Ed.). "Corrosion of aluminum and aluminum alloys". Asm International, (1999).
- [20] Chandra, B. T., & Shivashankar, H. S. 'Effect of heat treatment on hardness of Al7075-Albite particulate composites'. Materials Today: Proceedings, 4(10), 10786-10791, (2017).
- [21] J. R. avis, "Aluminum and Aluminum alloys", ASM Specialty Handbook, Metals Park USA, (1994).
- [22] I.J. Polmear, "Light Alloys", E. Arnold, Hodder& Stoughton Ltd. UK, Third Edition, (1995).
- [23] C ,Flament. "Etude des évolutions microstructurales sous irradiation de l'alliage d'aluminium 6061-T6". Doctoral dissertation. Université Grenoble Alpes, (2015).
- [24]. C, Vargel. "Corrosion of Aluminium, Elsevier". (2004).
- [25]. J, E, Hatch. "Aluminium; properties an physical metallurgy", American society for metals, 242-315, (1984).
- [26]. M.YAKOUBI;" Effet des petites déformations par compression Sur le comportement à la corrosion de l'alliage d'aluminium de fonderie Al 4½Cu". Mémoire de magister,
- Université Mouloud Mammeri Tizi-Ouzou Algérie, (2015).
- [27]. N.KHELLAF. "Effet des traitements de vieillissement sur le comportement électrochimique de l'alliage Al-Mg3 (AA5754) dans une solution aqueuse de 3.5% NaCl ". Mémoire de master. Université Mohamed Khider de Biskra,(2019).
- [28]. O.YOUSFI, & M.LABID. 'Etude de l'efficacité de l'inhibiteur de corrosion NORUST IG 514 dans les installations pétrolières du champ rhoud baguel 'Mémoire e de master. Université Ouargla, (2022).
- [29]. D.KHERBICHE, & Y.KEMER. "Etude des causes de la

- corrosion des bacs de stockage de pétrole. Ecole Nationale Supérieure des Mines et de la Métallurgie. Mémoire de master .UV Annaba (2020)
- [30]. B.KORICHI. "Etude et caractérisation de la corrosion des alliages d'Aluminium-
- Silicium". Thèse de Doctorat en Sciences.UV TIZI-OUZOU, (2024)
- [31]. S.BENTAALLA, & A.BETIT. "Caractérisations électrochimiques de l'acier inoxydable
- (18% Cr) et l'acier au carbone (X59) utilisés dans le l'industrie pétrolière'. Mémoire de master. M'hamed Bougara faculté des sciences ,(2020).
- [32]. N.Bernard , N.Pébére, C.Richard , & M.Wery . "preventation et lutte contre la
- corrosion, Chapitre I : La corrosion dans l'industrie Pétrolière". UMBB 2019/2020 28 lausanne, 755, (2004).
- [33]. C.Chinogurei. "Propriétés inhibitrices de l'huile de cade sur la corrosion de l'aluminium.". *Diplôme de Master, Université de Badji Mokhtar, Annaba*, (2018). [34]. C. Fiaud, «Inhibiteurs de corrosion M160». Technique de l'ingénieur, (2000).
- [35]. Bommersbach, P., Alemany-Dumont, C., Millet, J. P., & Normand, B. Electrochemical Characterization of a corrosion inhibitor: influence of temperature on the inhibition mechanism. In *Meeting Abstracts* (p. 239),(2005).
- [36]. G. W.F.WAYNE, «Green inhibitors development and applications for aqueous systems,» chez Corrosion, Nace International Houston, TX, Schlumberger, , p.

Paper n° 04407,(2004)

- [37]. Z.BENGUESMI . "Etude de la corrosion de l'alliage d'aluminium (2024 T3) dans un milieu basique (NaCl)". Mémoire Pour obtenir le diplôme de master. ENP,(2012).
- [38]. M.R ABDEDDAIM, & A. BENDALIBRAHAM. '' Etude du comportement électrochimique d'un alliage d'aluminium Al6061 à différentes températures''. Mémoire Pour obtenir le diplôme de master.ENP,(2020).
- [39]. B, JO'M, & L. V Minevski, "On the mechanism of the passivity of aluminum and aluminum alloys". *Journal of Electroanalytical Chemistry*, 349(1-2), 375-414,(1993).
- [40]. K.SORAY. ''Elaboration et étude de la corrosion des alliages Al-Zn et Al-Zn-Sn dans une solution à 3% en poids de NaCl''. Thèse

- Magistère. Université Mouloud Mammeri de Tizi Ouzou, (2004).
- [41] K. Wefers & C. Misra, "Oxides and hydroxides of aluminium". ALCOA Laboratories, (1987).
- [42]. A .Younis, M. M. B, El-Sabbah,., & R ,Holze,. The effect of chloride concentration and pH on pitting corrosion of AA7075 aluminum alloy coated with phenyltrimethoxysilane. *Journal of Solid State Electrochemistry*, 16, 1033-1040,(2012). [43]. K. Wefers, & C .Misra. ''Oxides and hydroxides of aluminum ''.(Vol. 19, pp. 1-
- 92). Pittsburgh, PA: Alcoa Laboratories, (1987).
- [44]. P. M, Huang, M. K, Wang, N .Kämpf,., & D. G, Schulze. ''Aluminum hydroxides. *Soil mineralogy with environmental application*''s, 7, 261-289,(2002).
- [45]. C. Vargel. "Corrosion of Aluminium", Elsevier, (2004).
- [46] . V .Vujicic, B. Lovrecek. "Properties of boehmitized aluminium surface". Surface technology 17, 29-35, (1982).
- [47] S .Bertling." Identification of thin surface films on aluminium with FTIR spectroscopy". Swedish institute for metals research, ISSN 0284-2378, (1995).
- [48] .S. Iijima, T. Yumura, and Z. Liu, 'One-dimensional nanowires of pseudoboehmite (aluminum oxyhydroxide γ-AlOOH)', Proc. Natl. Acad. Sci. U. S. A., vol. 113, no. 42, p. 11759, Oct. (2016).
- [49].Y.-P. Lee, Y.-H. Liu, and C.-S. Yeh, "Formation of bayerite, gibbsite and boehmite
- particles by laser ablation", Phys Chem Chem Phys, vol. 1, pp. 4681–4686, Jan. (1999).
- [50].J. I Goldstein, D. E Newbury, J. R. Michael Ritchie, N. W Scott,
- J. H. J, & D. C Joy. "Scanning electron microscopy and X-ray microanalysis". Springer, (2017).
- [51]. J. R. Davis (Ed.). "Corrosion of aluminum and aluminum alloys". Asm International, (1999).
- [52]. McCafferty, E. «Validation of corrosion rates measured by the tafel extrapolation method», Corrosion Science, 47(12),3202-3215, (2005).
- [53] R.Boulmerka. 'Etude de la corrosion des instruments chirurgicaux dentaires lors de la stérilisation 'Thèse de Doctorat . UV Annaba, (2012) .